PASSIVE NEUTRON DETECTION IN PORTS

FOR HOMELAND SECURITY APPLICATIONS

A Thesis

by

EOWYN ELISE PEDICINI

Submitted to the Office of Graduate Studies of
Texas A&M University
in partial fulfillment of the requirements for the degree of

MASTER OF SCIENCE

Approved by:

Chair of Committee,	William S. Charlton
Co-Chair of Committee,	Craig M. Marianno
Committee Member,	Arnold Vedlitz
Head of Department,	Yassin Hassan

May 2013

Major Subject: Nuclear Engineering

ABSTRACT

The smuggling of special nuclear material (SNM) has long been a concern. In April 2009, President Obama declared that a terrorist acquiring a nuclear weapon was the most immediate threat to global security. The Second Line of Defense (SLD) initiative was stood up by the National Nuclear Security Administration to deter, detect, and interdict illicit trafficking of nuclear and radioactive materials across international borders and maritime shipping. The SLD initiative does not provide for the detection of SNM being carried on small, personal watercraft.

Previous work examined the possibility of using active neutron detectors to induce fission in SNM and detect the response. This thesis examines the possibility of detecting SNM using passive ^{3}He neutron detectors. Monte Carlo N-Particle (MCNP) simulations were run to determine the best detector configuration. Detecting sources at increasing depths, detecting moving sources and the effects of waves were also simulated in MCNP. Comparisons with experimental measurements showed that detectors parallel to the surface of water were best at detecting neutron sources below the surface. Additionally, stacking detectors and placing a cadmium sheet between the polyethylene blocks resulted in a greater ability to determine the height of a source by taking the ratio of count rates in the lower and upper detectors. Using this configuration, a source of strength 3.39×10^{5} n/s could be detected to a depth of 12.00 in below the water surface. Count rates in the presence of waves did not average out to count rates taken above a flat plane of water. Detectors closer to the water performed worse than above a flat plane while detectors placed higher recorded more counts than above a flat plane. Moving sources were also simulated; sources under water, 3.00 ft from the detectors, and moving at 5.8 kts could be detected above background.

DEDICATION

This thesis is dedicated to my friends and family.

ACKNOWLEDGEMENTS

I would like to thank my co-chairs, Dr. Charlton and Dr. Marianno, for supporting me through this research. Dr. Marianno, I especially enjoyed coaching and playing soccer with you. It's rare to find other people who also appreciate soccer. Hopefully you learned something about neutrons. I would also like to acknowledge my committee member Dr. Vedlitz for his guidance.

Thank you to the staff at the Nuclear Science Center for allowing us to run experiments there. A special thanks to Jerry Newhouse for helping to facilitate the experiments and for agreeing to come in early to the NSC to monitor the experiments. Thank you to Dr. Solodov for his knowledge and advice on portal monitors, and for shepherding us in Russia and translating everything. Thank you to my fellow graduate students in NSSPI and nuclear engineering for making my experience at Texas A&M University memorable. Especially to Braden Goddard for his knowledge and expertise in neutron detection systems.

NOMENCLATURE

B	Boron
BF_3	Boron trifluoride
Cd	Cadmium
Cf	Californium
cps	counts per second
CsI	Cesium iodide
eV	electron volt
H	Hydrogen
He	Helium
HEU	Highly Enriched Uranium
IAEA	International Atomic Energy Agency
ITDB	IAEA Illicit Trafficking Database
Li	Lithium
MCNP	Monte Carlo N-Particle
NNSA	National Nuclear Security Agency/Administration
NSC	Nuclear Science Center
PNNL	Pacific Northwest National Laboratory
Pu	Plutonium
RPM	Radiation Portal Monitor
SLD	Second Line of Defense
SNM	Special Nuclear Material
SQ	Significant Quantity

TAMU	Texas A&M University
TRIGA	Training, Research, Isotopes, General Atomics
U	Uranium
WGPu	Weapons Grade Plutonium
Z	Atomic Number

TABLE OF CONTENTS

Page

LIST OF FIGURES

Page

Page

LIST OF TABLES

1. INTRODUCTION

The smuggling of special nuclear material (SNM) has long been a concern for homeland security. Between January 1993 and December 2011, 2164 incidents were reported to the International Atomic Energy Agency (IAEA) Illicit Trafficking Database (ITDB). Sixteen of those cases involved the unauthorized possession of either highly enriched uranium (HEU) or plutonium with several of the cases involving kilogram quantities of those materials [1].

Passive neutron detection using ^{3}He detectors is a nondestructive assay (NDA) technique used to detect neutrons produced from fission and (α,n) reactions. Neutrons produced from these sources are moderated to thermal energies with low-Z material where they can then be absorbed by ^{3}He, producing charged particles which can be detected.

The research presented here describes the use of passive neutron detectors to detect SNM while being smuggled into the country via small, personal watercraft. This section presents the previous work and provides a background on neutron detection, the Monte Carlo code used to simulate scenarios, and a description of the types of boats that are a concern. Section 2 describes the MCNP simulations run for this thesis. Section 3 presents the procedure and setup of the experiments occurring in November 2012. Section 4 provides a comparison of the experimental and simulation results, while section 5 details a discussion of the results of further simulations. Section 6 covers conclusions and future work in the use of passive neutron detectors for SNM detection in personal watercraft.

1.1 Motivation

The smuggling of SNM has long been a concern. With the breakup of the Soviet Union, lapses in safeguards and security resulted in a loss of accountability for an unknown amount of

SNM. Sixteen cases reported to the IAEA ITDB involved the unauthorized possession of either HEU or plutonium with several of the cases involving kilogram quantities of the material. [1] As an example, in the summer of 1994, Germany saw four instances of plutonium being smuggled through the country. Adolph Jaekle was found with 6 g of plutonium at his home in Tengen, Germany [2]. In a separate incident, a Columbian and two Spaniards were arrested at an airport in Munich, Germany with several hundred grams of plutonium and uranium oxides after having flown with the material from Moscow, Russia to Munich [3]. In 1992, an entire fuel assembly was stolen from the nuclear power plant in Ignalina in Lithuania. Of the 124 kg of 2% enriched UO_2, only 100 kg were later recovered [3].

In April 2009, President Obama declared that a terrorist acquiring a nuclear weapon was the most immediate threat to global security [4]. The Second Line of Defense (SLD) initiative was stood up by the National Nuclear Security Administration (NNSA) to deter, detect, and interdict illicit trafficking of nuclear and radioactive materials across international borders and by maritime shipping. SLD aims to equip 30 countries with portal detection equipment by 2018. Through the Megaports Initiative, the SLD also plans to equip more than 100 seaports with radiation detection equipment by 2018 with the goal of scanning 50% of global shipping traffic [5].

While the Megaports Initiative seeks to detect SNM being smuggled by maritime traffic, the intended target of this is cargo from large cargo ships. There is a gap in detection capability against small, personal watercraft, which could easily be used to carry a significant quantity (SQ) of SNM: 8 kg of plutonium or 25 kg of ^{235}U at enrichments greater than 20% [6]. Until September 11, 2001, much of the maritime strategy of the United States focused on large commercial vessels. Concern with small vessels was traditionally reserved for safety and basic law enforcement issues. The Department of Homeland Security defines small vessels as any

watercraft less than 300 gross tons, regardless of the method of propulsion [7]. Gross tonnage is a function of the volume of the ship's enclosed spaces; these vessels are often less than 30.5 m (100 ft) in length. Examples of small vessels include sailboats, fishing boats, recreational boats, and yachts. In 2008, there were nearly 13 million registered US recreational vessels, 82,000 fishing vessels, and 100,000 other small commercial vessels [7]. These are the same types of craft used to smuggle tons of drugs into the United States per year. Additionally, the challenges faced by detecting SNM on small personal watercraft are different from the challenges faced detecting material being driven into the country. While all vehicles must drive slowly through radiation portal monitors (RPMs) placed on roads, boats are less restricted in their direction of motion and speed, making it more difficult to detect illicit material onboard. There is also no guarantee a boat will drive past detectors at speeds slow enough for SNM to be detected.

The SLD initiative utilizes both gamma and neutron detection systems to detect illicit trafficking. Much of the focus has been on gamma detection systems because gamma rays are produced by most sources of concern for illicit trafficking [8]. However, plutonium, which can be used in improvised nuclear devices, also emits significant amounts of neutron radiation, mostly coming from ^{240}Pu, which has a fission yield of 1.02×10^{3} n/s·g [9]. For a significant quantity (SQ) of metallic plutonium, assuming 5% ^{240}Pu and taking into account neutron multiplication, 8.73×10^{5} n/s would be emitted from the ^{240}Pu. Advantages of neutron detection over gamma detection include a low natural background (0.012 n/cm^2·s at sea level) and few neutron sources being carried commercially [10]. Conversely, highly enriched uranium (HEU) is difficult to detect because it emits few neutrons (^{238}U has a fission yield of 1.36×10^{-2} n/s·g) and emits low energy gamma rays which can be easily shielded [9].

1.2 Objectives

The objective of this research was to investigate detectors capable of detecting SNM in small watercraft before it can be smuggled into the country. To utilize this, a further understanding of the neutron spectrum from a water-air interface was necessary. For this project, ^{3}He detectors were used to determine the best configuration for detecting neutrons near a water/air interface. Simulations were benchmarked against experimental measurements taken at the Nuclear Science Center (NSC) at Texas A&M University. Additional simulations were run to characterize detector response to moving sources and in the presence of waves of various sizes.

1.3 Previous Work

Klaus-Peter Ziock et al. investigated methods to detect SNM in personal watercraft using gamma detection systems [11]. This method involves using cesium iodide (CsI) detectors with a coded aperture, which uses a lead screen to shield the detector from gamma rays. This pattern of blocking and unblocking the detectors from incident gamma rays reduces the background counts and strengthens a weak signal. This method was previously tested on roads, and a feasibility study was conducted to see if the system could be adapted to marine environments. A 5 mCi ^{137}Cs source could be detected at a range of 20 m for vessels traveling between 2 and 6 kts (1 to 3 m/s). This system also relies on cameras to identify and track targets, and more work is needed to track a greater number of targets as well as targets going past the detector.

Former Texas A&M University graduate student Norman Johansen's master's thesis studied the use of active detection techniques to detect SNM in small watercraft [12]. Pulsed neutron generators emit neutrons which can be used to induce fission in uranium and plutonium;

the neutrons emitted from fission can then be detected. Using MCNP, he found that active interrogation could be used to detect the presence of both plutonium and uranium sources while not exposing passengers to high doses. However, he also found that the passive neutron signature from plutonium was much stronger than the active signature, though the active signature from uranium was much stronger than the passive signature.

Increased neutron counts are unusually registered around large sources of water, such as oceans. Water is an effective moderator of neutrons. Near air/water interfaces, cosmic-ray neutrons have a higher thermal flux and lower fast flux than seen in free air [13]. Additionally, the neutron flux near an air/steel interface has been observed up to 25 times the flux at an air/water interface [14]. Around large ships, elevated neutron count rates are observed due to the production of spallation neutrons from cosmic rays striking the metal in the ship [15]. This is called the "ship effect;" unfortunately, there are few open-source publications about the ship effect. Ship effect neutron rates are dependent on latitude, altitude, weather, and solar activity. However, personal watercraft are too small to elicit this reaction, as this is observed around tens of tons of high-Z material [16].

Due to their large absorption cross section, ^{3}He detectors are one of the best passive neutron detectors. However, following the terrorist attacks of September 2001, the increase in demand for ^{3}He detection systems has outpaced the supply. Richard Kouzes et. al at Pacific Northwest National Laboratory reviewed alternative neutron detectors to replace the use of ^{3}He and ultimately found that while several detection systems can come close to the detection abilities of ^{3}He systems, none can match it [17]. For instance, using boron trifluoride (BF_3) tubes with boron enriched to 90% ^{10}B requires three detectors to match the detection capabilities of one ^{3}He tube. Along with requiring three times as many detectors, BF_3 is a toxic gas, posing an additional hazard if it were to leak.

1.4 Theory

1.4.1 Passive Neutron Detection

Neutrons are neutral particles and do not interact in matter through the coulomb force. Due to their lack of charge, neutrons can pass through materials without interacting, making it impossible to directly detect them. Unlike gamma rays, neutrons do not interact with the electrons of an atom but rather with the nucleus. Neutrons can be detected by their interactions with nuclei, which produce secondary radiations, often in the form of heavy charged particles. Neutrons are produced from fission and from nuclear reactions, such as (α,n) or (γ,n) reactions. Neutrons produced from fission are born with a distribution of energies. This distribution is described by a Watt spectrum. Figure 1 shows the prompt neutron spectrum from the spontaneous fission of ^{252}Cf, which has a mean neutron energy of 2.14 MeV [9]. The prompt neutron spectrum of ^{252}Cf is similar to that of ^{240}Pu and is frequently used as a test source for neutron detection experiments. As can be seen, most neutrons are born in the fast spectrum with energies greater than 1 MeV.

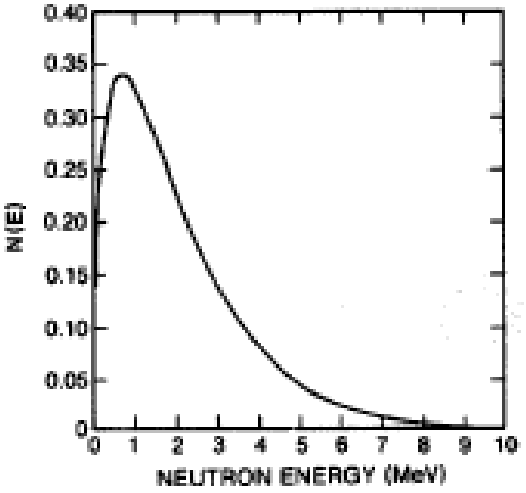

Figure 1. Spontaneous fission neutron spectrum of ^{252}Cf [9]**.**

Table I shows the spontaneous fission yield from neutron sources of interest. As can be seen, uranium isotopes emit relatively few neutrons per gram. ^{238}U, the primary uranium isotope of interest, emits only 1.36×10^{-2} n/s·g. Even in HEU, ^{238}U will be the primary neutron emitter. Plutonium isotopes emit more neutrons, particularly ^{240}Pu, present in small quantities in weapons grade plutonium. Also of note is the spontaneous fission yield of ^{252}Cf, which emits 2.34×10^{12} n/s·g [9].

Table I. Spontaneous fission yield from common neutron sources [9]**.**

Isotope A	Protons Z	Neutrons N	Half-Life	Fission Yield (n/s-g)	Spontaneous Multiplicity	Thermal Multiplicity
^{232}Th	90	142	1.41×10^{10} y	$>6 \times 10^{-8}$	2.14	1.9
^{232}U	92	140	71.7 y	1.3	1.71	3.13
^{233}U	92	141	1.59×10^{5} y	8.6×10^{-4}	1.76	2.4
^{234}U	92	142	2.45×10^{5} y	5.02×10^{-3}	1.81	2.4
^{235}U	92	143	7.04×10^{8} y	2.99×10^{-4}	1.86	2.41
^{236}U	92	144	2.34×10^{7} y	5.49×10^{-3}	1.91	2.2
^{238}U	92	146	4.47×10^{9} y	1.36×10^{-2}	2.01	2.3
^{237}Np	93	144	2.14 x 106 y	1.14×10^{-4}	2.05	2.70
^{238}Pu	94	144	87.74 y	2.59×10^{3}	2.21	2.9
^{239}Pu	94	145	2.41×10^{4} y	2.18×10^{-2}	2.16	2.88
^{240}Pu	94	146	6.56×10^{3} y	1.02×10^{3}	2.16	2.8
^{241}Pu	94	147	14.35 y	5×10^{-2}	2.25	2.8
^{242}Pu	94	148	3.76×10^{5} y	1.72×10^{3}	2.15	2.81
^{241}Am	95	146	433.6 y	1.18	3.22	3.09
^{242}Cm	96	146	163 d	2.10×10^{7}	2.54	3.44
^{244}Cm	96	148	18.1 y	1.08×10^{7}	2.72	3.46
^{249}Bk	97	152	320 d	1.0×10^{5}	3.40	3.7
^{252}Cf	98	154	2.646 y	2.34×10^{12}	3.757	4.06

Most neutron detectors, including those used in this project, detect thermal neutrons, which have an energy around 0.025 eV. In order to moderate neutrons to this energy, the detector is often surrounded with a low-Z material, such as the hydrocarbon polyethylene, $(C_2H_4)_nH_2$. A neutron can lose almost all its energy in a single interaction with a hydrogen

nucleus because they are of similar mass. Neutrons elastically scatter off the moderator material, losing energy with each interaction. Neutron detectors typically do not preserve the energy information of the incident neutron. Because of this, and the distribution of energies neutrons are born with, isotope identification using these neutron detectors is not possible as it is with gamma detectors. However, this is mitigated by the relatively few neutron sources in commercial shipping, such as those used for soil and concrete moisture measurements and well logging sources.

Neutrons are detected through interactions with materials that have high absorption cross sections. After a nucleus absorbs a neutron, it emits secondary radiation which can then be detected. These absorption cross sections decrease with increasing neutron energy. A common neutron detector is ^{3}He, which is rare, constituting only about 0.00014% of helium in nature. It is a stable isotope produced from the decay of tritium, ^{3}H, which has a half life of 12.32 years. Tritium can be produced from the neutron activation of ^{6}Li targets. Current supplies of ^{3}He come from the decaying ^{3}H in the weapons stockpile. The absorption cross section for ^{3}He, which is the dominant interaction in ^{3}He for neutrons below energies of 10 keV, can be seen in Figure 2 [18]. Around 0.025 eV, the energy of thermal neutrons, the absorption cross section is around 5000 b. For ^{3}He detectors, ^{3}He absorbs a neutron and emits a proton and a triton, which can be detected:

$$^{3}_{2}\mathrm{He} + ^{1}_{0}\mathrm{n} \rightarrow ^{3}_{1}\mathrm{H} + ^{1}_{1}\mathrm{p} \qquad \text{Eq. 1}$$

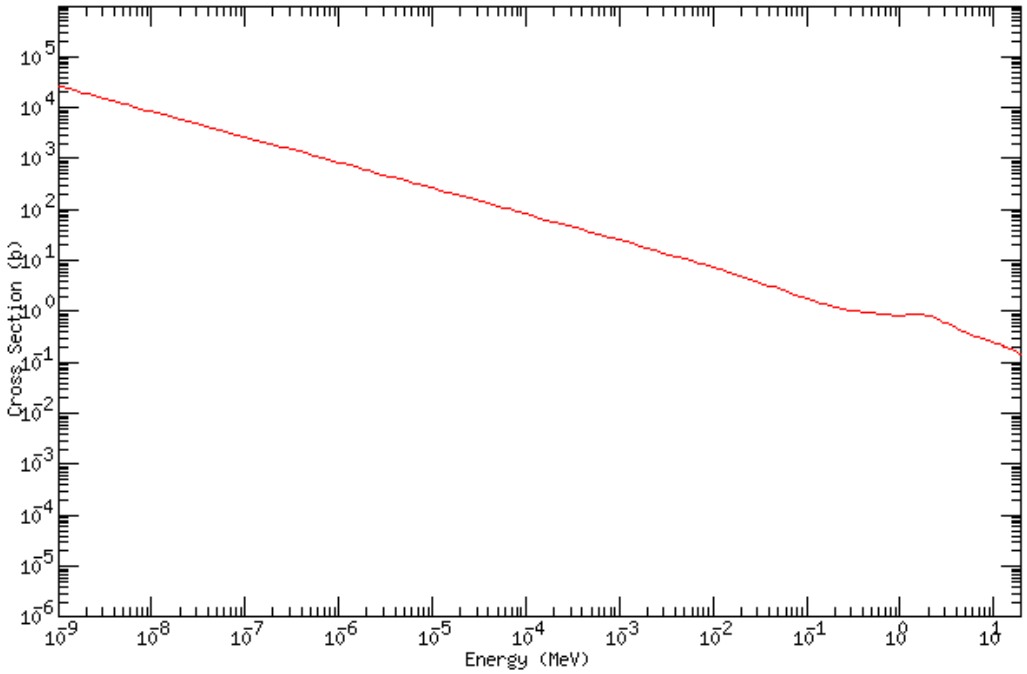

Figure 2. The absorption cross section of ^{3}He [18]**.**

Neutrons produced from fission are emitted isotropically from the source. Unless a detector has 4π coverage around a source, only a fraction of neutrons emitted from SNM will interact inside a detector. This probability decreases by $1/r^2$ as the source-to-detector distance in a vacuum increases. It is not feasible to have 4π coverage in the scenario of detecting neutrons on watercraft as this geometry requires a stationary and relatively small source. Correspondingly, the geometric efficiency, the solid angle the detector encompasses around a source, will be low.

1.4.2 MCNP

MCNP is a general-purpose Monte Carlo code that can be used for neutron, photon, electron, or coupled neutron-photon-electron transport [19]. The Monte Carlo method is a calculation technique that relies on repeated random sampling to predict the behavior of a system. Instead of trying to predict how an individual neutron interacts, Monte Carlo methods

calculate how a fraction of a large population of neutrons interacts. Neutrons are created at a certain location and energy, and travel distances consistent with their mean-free-path lengths in the material. At the end of each step, an interaction is selected based on the cross section of the interaction of interest in the material. These interactions are followed until there are no further interactions of interest, such as the neutron leaks out of the system, or is absorbed. If the neutron is involved in a multiplication event, the resulting neutrons are each followed. By repeating this process for large numbers of neutrons, average behaviors and their associated uncertainties can be determined.

Several types of tallies can be used in MCNP. Both f4 and f8 tallies were used in this project. An f4 tally is the average cell flux tally and counts the particle track lengths, or distances traveled by each particle, through a cell volume. The units of an f4 tally are particles/cm^2. Energy bins were created on a lethargy scale, ranging from $1x10^{-8}$ MeV to $1x10^{2}$ MeV. The f4 tally was used to determine the neutron spectrum in the detectors. Because ^{3}He detectors have a higher absorption cross section and thus a higher efficiency in the thermal spectrum, it was important to determine if enough neutrons were thermalized prior to entering the detectors.

An f8 tally is a pulse height distribution. The f8 tally was separated into specific energy bins ranging of 0 MeV, 1 eV, 100 keV, and 10 MeV. The units of an f8 tally are pulses. In order to convert an f8 tally into count rate (s^{-1}), it must be multiplied by the activity of a source. For this research, a source activity of $3.39x10^{5}$ n/s was used, as this was the activity of the ^{252}Cf source on hand at the time of the measurements. The f8 tally was used to determine the count rate in the ^{3}He detectors.

2. SIMULATIONS

The following section details the MCNP simulations performed in this work. These simulations were used to determine the best detector configuration for a neutron source below the water, as well as characterize the detector response to neutrons at increasing depths below the surface of water, moving neutron sources, and the effect of waves on neutron detection.

2.1 Materials Used

The detectors used in this simulation were the LND Inc. Model 252 ^{3}He cylindrical detectors [20]. The detectors were 28.45 cm long, 1.00 in (2.54 cm) in diameter, have an aluminum casing, and are at a pressure of 4 atm. An increase in pressure is attained by having more ^{3}He gas in the tube; the increased number of ^{3}He atoms increases the chances of interaction with a neutron and thus have a higher efficiency. These detectors were placed in polyethylene blocks 12.00 in (30.48 cm) long, 6.00 in (15.24 cm) wide, and 2.00 cm (5.08 cm) tall. Each polyethylene block could hold two detectors placed 4.00 in (10.16 cm) apart. The detectors were placed 1.00 in (2.54 cm) above a plane of fresh water.

For some simulations, a 2 mm block of cadmium was placed between the polyethylene blocks. The large absorption cross section of ^{113}Cd at thermal energies means it absorbs neutrons at energies below 1 eV. Figure 3 shows the absorption cross section of ^{113}Cd and natural cadmium at energies between 0.001 eV and 10 MeV [18]. By selectively shielding some detectors in an array from thermal neutrons coming from a specific direction, a difference in count rate is expected between the shielded and unshielded detectors. The background is expected to be similar in all detectors, so higher count rates in some detectors could indicate the location of a neutron source relative to the detectors. For these experiments, a cadmium sheet

was placed either between detectors of different heights to determine source height or between detectors at different lateral positions to determine the lateral position of a source.

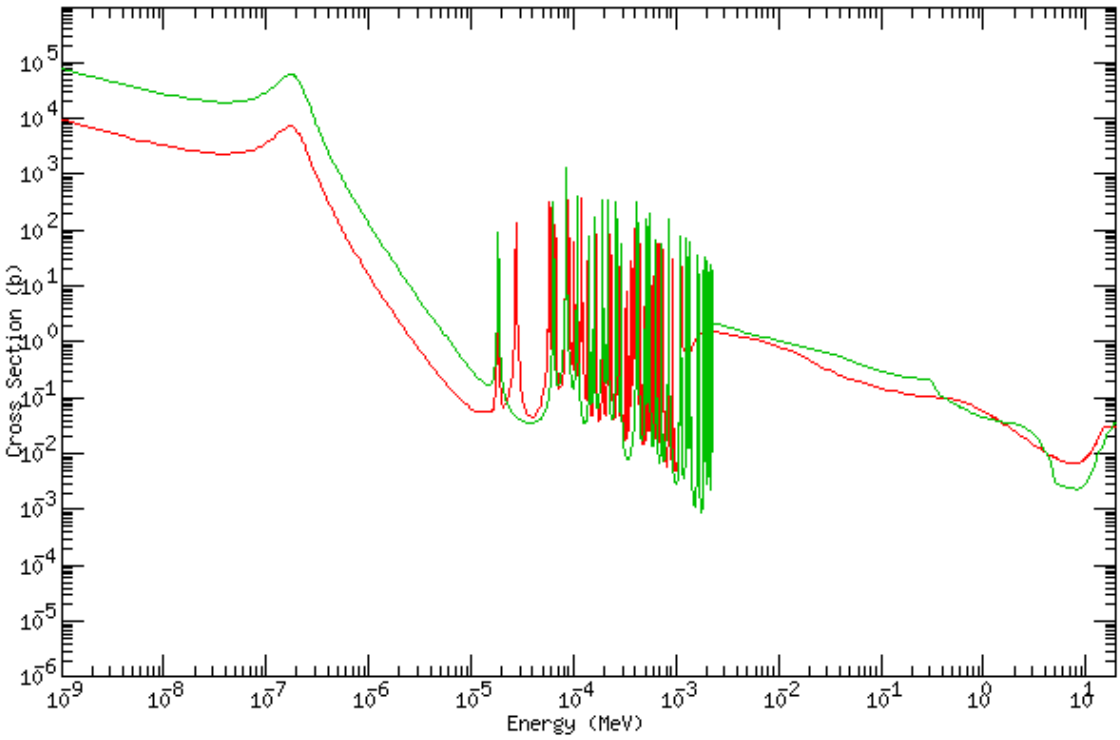

Figure 3. Absorption cross section for ^{113}Cd (green) and natural cadmium (red) [18]**.**

Fresh water was used because it could be compared to the experimental results. The average salinity of open ocean water is 0.00035 g/cm^3, with water in ports ranging from 0.00031 to 0.00036 g/cm^3. Sea water will have other ions compared to fresh water, most prominently chloride, sodium, and magnesium. These ions all have low absorption cross sections; the absorption cross section for chlorine is three orders of magnitude lower than that of cadmium, and the absorption cross sections for sodium and magnesium are even lower. Thus it is expected that results using fresh water will be nearly identical to those using sea water.

2.2 Background Count

First, a background simulation was run. Background neutrons are present in the atmosphere from the interaction of cosmic rays from matter, as well as the decay of naturally occurring radioactive material. At sea, the contribution to the neutron background from naturally occurring sources is not significant. Two polyethylene blocks, each with two detectors, were stacked and placed parallel to a plane of water as can be seen in Figure 5a on page 15. A distributed neutron source was placed at the surface of a sphere with a radius of 100 cm. The sphere was surrounding the detectors. The neutron source was isotropically emitted from the sphere. Inside the sphere was a body of water in the lower-half space and a volume of dry air in the upper-half space The sphere was sized such that the source neutrons could interact with the air and water in ways they ordinarily would in the real world. The neutrons were given a ^{252}Cf energy spectrum. An f4 tally was used to determine the neutron flux inside the neutron detectors. This was converted into a count rate using:

$$CR = \overline{\varphi}\overline{\sigma}_a NV \qquad \text{Eq. 2}$$

where $\overline{\varphi}$ is the neutron flux averaged over all thermal energies (n/cm^2·s), $\overline{\sigma}_a$ is the absorption cross section for ^{3}He averaged over all thermal energies (cm^2), N is the number density of ^{3}He (atoms/cm^3), and V is the volume of the detectors (cm^3). N is calculated using:

$$N = \frac{\rho N_a}{A} \qquad \text{Eq. 3}$$

Here, ρ is the density of ^{3}He at 4 atm (in atoms/cm^3), N_a is Avogadro's number (6.022x10^{23} atoms/mol), and A is the atomic mass of ^{3}He, which is 3.01603 g/mol.

2.3 Configurations

Once the background neutron count rate was determined, a point source was modeled and several detector configurations were simulated. Each detector configuration was run both with and without a cadmium sheet placed between the polyethylene blocks. The detector configurations were all placed 21.00 in (53.34 cm) above a plane of water. For each configuration, the point source was placed 1.00 in (2.54 cm) below the surface of the water, even with the front face and centered on the detectors. The source was also placed in two other locations: 1.0 0in (2.54) cm below the surface of the water and directly to the right side of the detectors, and 16.00 in (40.64 cm) above and to the right side of the detectors. These source locations were kept the same for all simulations. These three locations are shown in Figure 4.

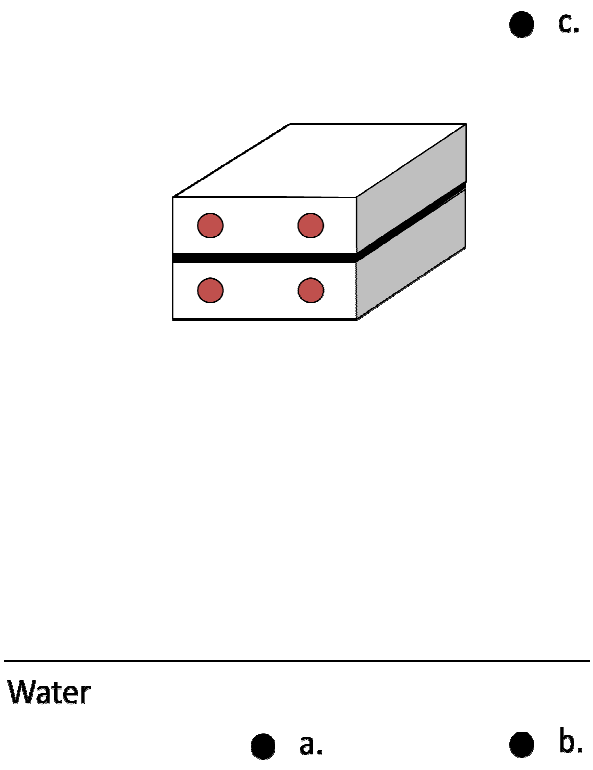

Figure 4. 4a. The location of a source placed directly below the detectors. 4b. The location of a source placed below and to the side of the detectors. 4c. The location of a source placed above and to the side of the detectors.

2.3.1 Parallel Configurations

Three different simulations were run with the detectors parallel to the surface of the water. In the first, four detectors were used. Two detectors each were placed in stacked polyethylene blocks, as can be seen in Figure 5a. This configuration was simulated both with and without a cadmium sheet between the polyethylene blocks. In the next simulation, only two detectors were used. These detectors were placed in a polyethylene block, while another polyethylene block without detectors was placed above the detectors (Fig. 5b). In the final simulation, two detectors were placed in a polyethylene block, which was stacked on top of another empty polyethylene block (Fig. 5c).

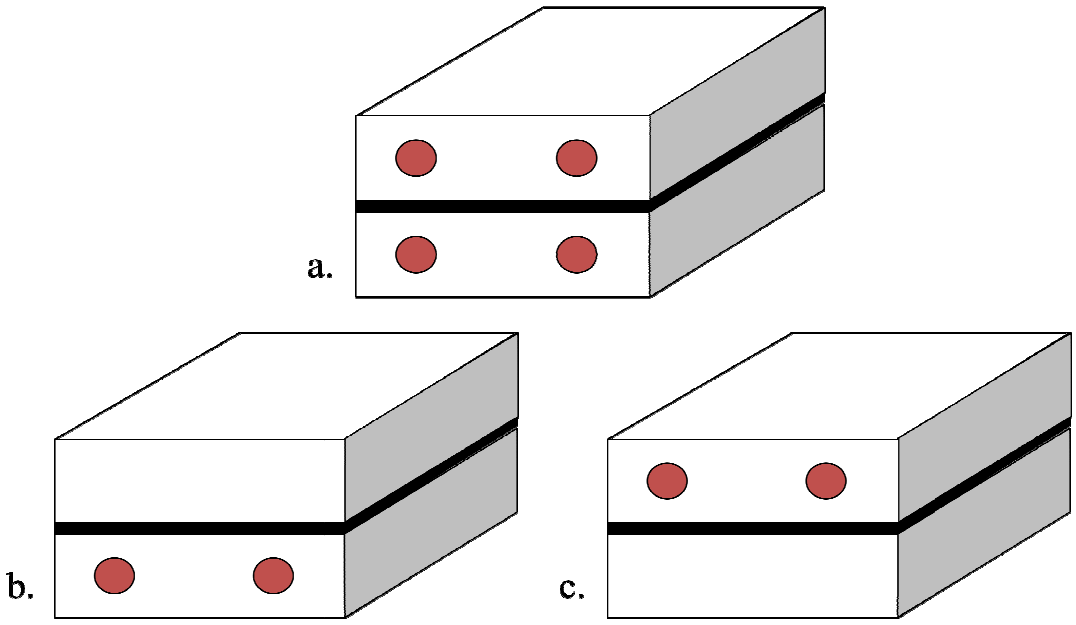

Figure 5. 5a. A view of 4 detectors (shown in red), with a cadmium sheet (black) between the polyethylene blocks. 5b. Two detectors in only the lower polyethylene block. 5c. Two detectors in only the upper polyethylene block.

2.3.2 Perpendicular Configurations

Two simulations were run with the detectors perpendicular to the surface of the water. In the first, four detectors were used. Two detectors each were placed in polyethylene blocks that were stacked next to each other (Fig. 6b). This configuration was simulated both with and without a cadmium sheet between the polyethylene blocks. In the next simulation, only two detectors were used. These detectors were placed in a polyethylene block perpendicular to the water surface and were above a polyethylene block placed parallel to the surface of the water (Fig. 6a). Again, the simulations were run both with and without a cadmium sheet.

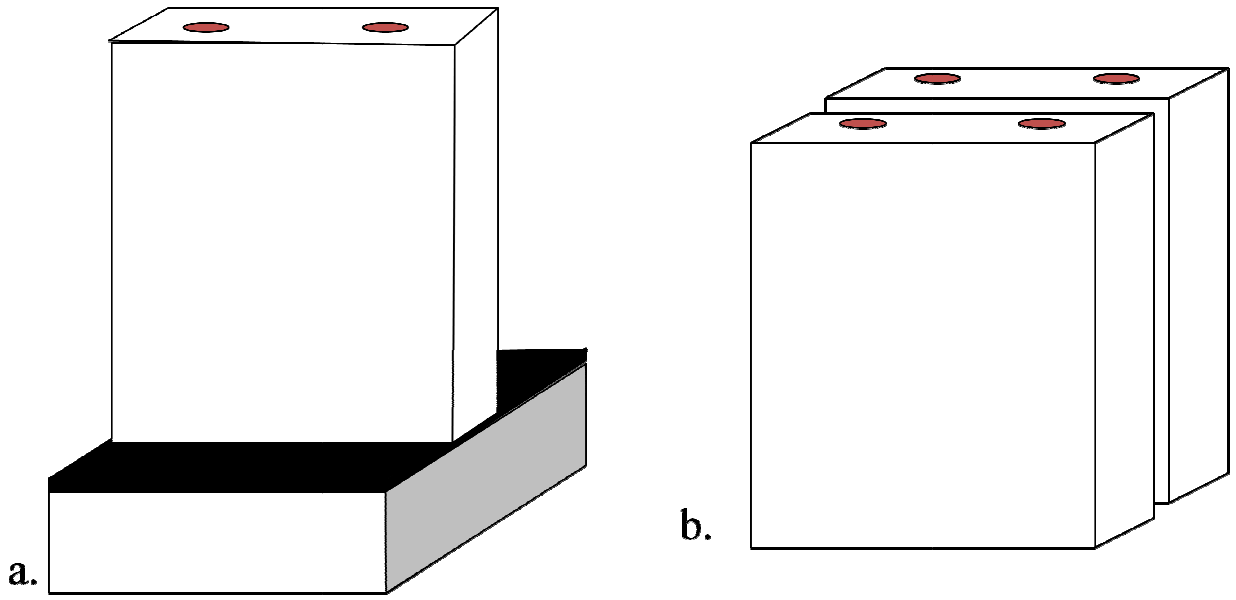

Figure 6. 6a. Two detectors perpendicular to the surface of water, stacked above a polyethylene block. 6b. Four detectors perpendicular to the surface, shown here without a cadmium sheet.

2.4 Depth Measurements

The two four-detector configurations, one parallel to the surface of the water and one perpendicular to the surface, were used for depth measurements. For both of these simulations, the cadmium sheet was placed between the polyethylene blocks. A ^{252}Cf source was simulated at various depths directly below the detectors, shown in Figure 7. The source was placed 3.00 in (7.62 cm) below the surface of the water and at 3.00-in intervals below that down to a final depth of 21.00 (53.34 cm). The purpose of the depth simulations was to determine the depth at which neutron sources could be detected.

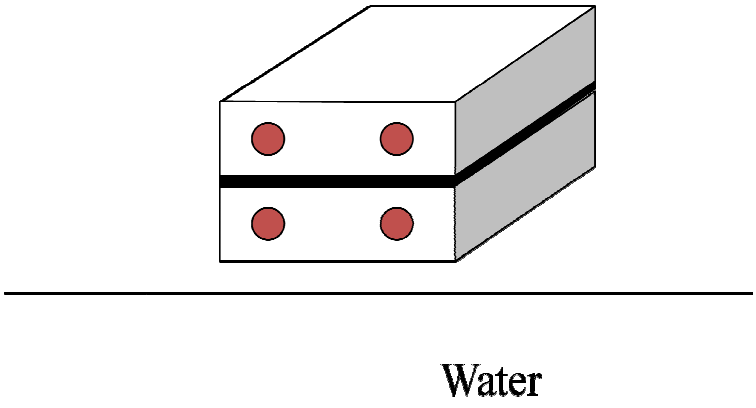

Figure 7. Source placed at increasing depths below the detectors.

2.5 Moving Sources

Several simulations were run with a moving source a distance from the two four-detector configurations (5a and 6b). MCNP is not capable of simulating a moving source directly, so a series of stationary simulations were run. Each of the stationary simulations can be converted into a count rate, which, when multiplied by a change in time, Δt, could be used to determine the total counts per source location:

$$C_i = CR_i \times \Delta t_i \qquad \text{Eq. 4}$$

The change in time (Δt_i) is acquired by dividing the distance of the interval (Δd_i) by the magnitude of the source velocity (v). The total counts for a source are then simply the summation of a series of counts for each location:

$$\sum C_i = \sum CR_i \times \Delta t_i \qquad \text{Eq. 5}$$

By knowing the activity of the source, the maximum detection velocity V could be calculated. As the velocity of the boat increases, Δt decreases, resulting in fewer counts registered. A threshold count rate can then be set at 1.5 cps, which is 3σ above the background count rate. This is the typical alarm threshold; counts below this are regarded as normal fluctuations while count rates above this threshold would result in an alarm.

The ^{252}Cf source was simulated both 6.00 in above and 1.00 in below the surface of the water and was placed at various locations on a line 1.00 ft (30.48 cm) away from the detectors. These simulations were run for lines running in both directions on the plane of the water, referred to as the x-direction and the y-direction. This was repeated for sources 2.00 ft (60.96 cm), and 3.00 ft (1.44 cm) away (Figure 8).

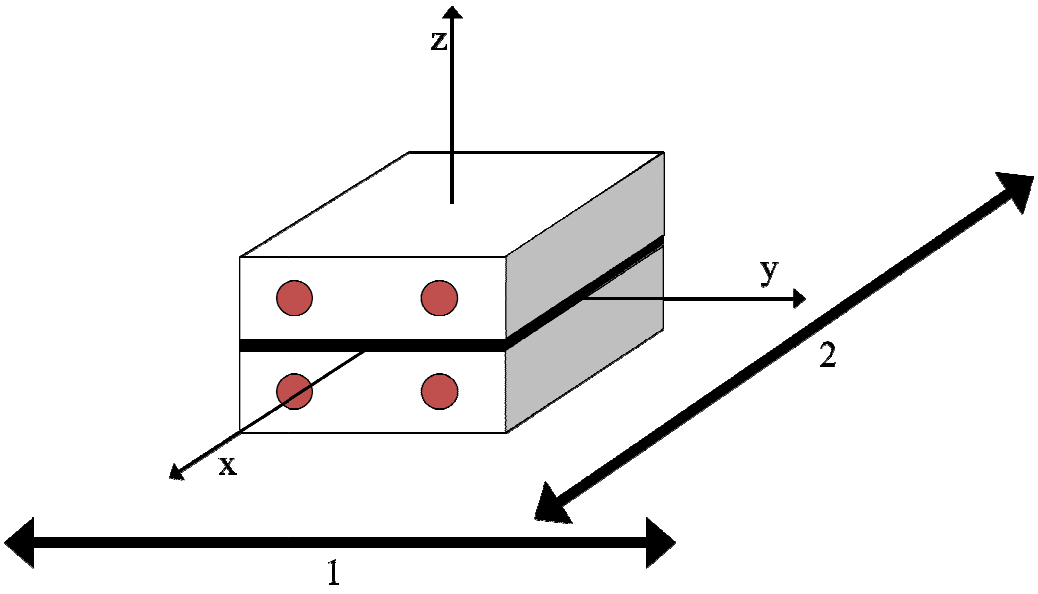

Figure 8. Depiction of moving sources. Line 1 demonstrates sources moving in the y direction at constant x, while 2 shows sources moving in the x direction at constant y.

2.6 Wave Simulations

The purpose of the wave simulations was to model the behavior of a neutron source in the hull of a boat, where the source could be alternating between being below and above the surface of the water. The waves simulations will be used to compare how neutron detection is affected by the air/water interface. Neutron count rates are much different in air and water, with the thermal flux rate much higher and the fast flux much lower near the interface than observed in free air [13] [21].

Several simulations were run to model the behavior of waves on neutron detection. These simulations were run with four detectors parallel to the surface of the water with a cadmium sheet placed between the polyethylene blocks. A ^{252}Cf source was placed at a location 3.00 in (7.62 cm) below the plane of water, but the water was given a series of cylindrical-shaped waves, as shown in Figure 9. The waves were given a radius of 3.00 in (7.62 cm), 6.00

in (15.24 cm), 9.00 in (22.86 cm), and 12.00 in (30.48 cm). The source was placed at eight equally spaced locations in a wave period, covering both the peak and trough of a wave. These locations can be seen in Figure 9.

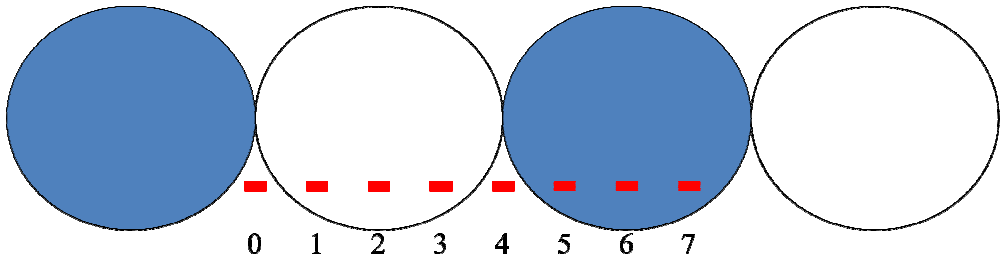

Figure 9. Here, the white circles represent air and the blue circles represent water. The source was placed at each of the eight numbered locations to cover a wave period.

For each wave size, four different simulations were run. The detectors were initially placed 1.00 in above the top of the wave. This configuration will later be referred to as "directly above the wave." Placing the detectors directly above the wave replicates the situation in which detectors would be placed on buoys or some other floating device. The detector height would fluctuate depending on the strength of the waves, but would remain a relatively constant height above the water. For the second configuration, the detectors were placed 24.00 in (60.96 cm) above the centerline of the waves, regardless of wave height. Detectors in this position will be referred to as "high above the water." Keeping the detectors a constant height above the plane of water models a situation in which the detectors would be mounted on a bridge, dock, or other stationary object. In this situation, the detector position is independent of the wave height and does not change regardless of wave strength. These configurations can be seen in Figures 10 and 11, respectively. The source and detectors were then moved in tandem to the eight previously mentioned positions, and the detectors remained directly above the source for each new source

location. For the other set of simulations, the source was kept in a constant location while the detectors were moved to the eight original locations, as shown in Figure 12. Keeping the source stationary, detectors were placed both directly above the waves and high above the water as before. This was to model the situation in which a source was moving relative to the detector location.

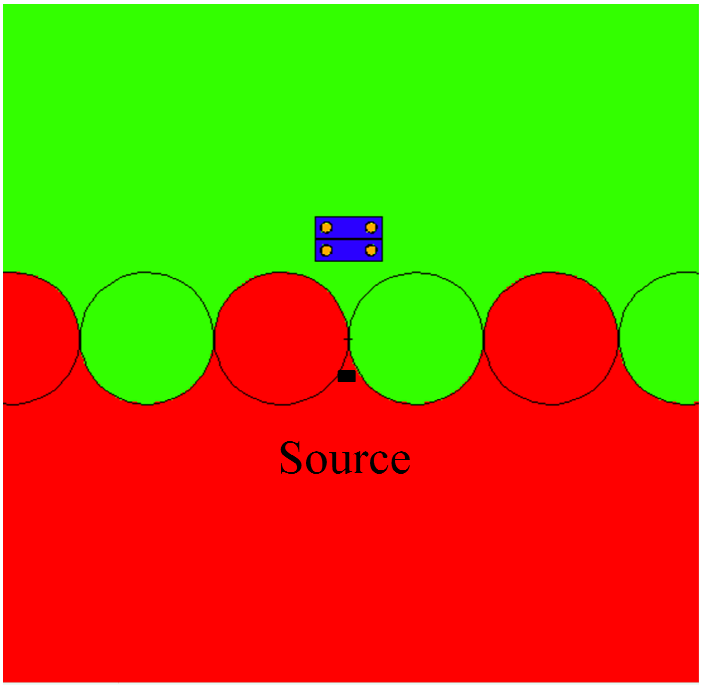

Figure 10. The detectors placed directly above the peak of the waves.

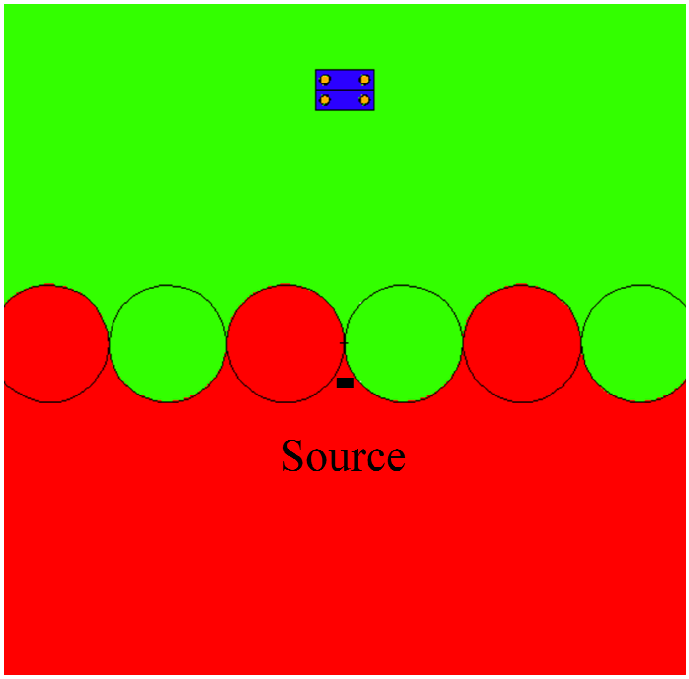

Figure 11. The detectors placed a constant height, 60.96 cm above the plane of the water.

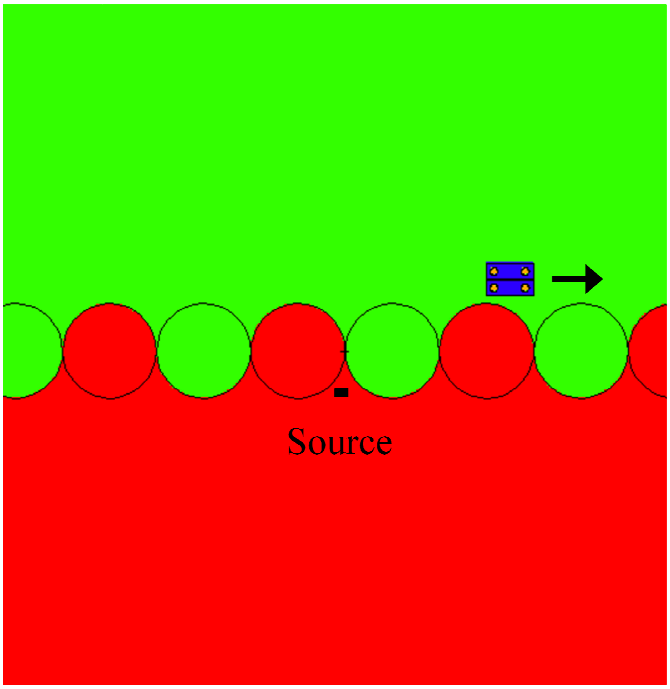

Figure 12. The detectors were moving relative to the source, which was held in the same location.

3. EXPERIMENTAL DETAILS

The following section details the experiments performed at the Nuclear Science Center (NSC) reactor pool at Texas A&M University on 29 and 30 November 2012. These experiments were run to test the different detector configurations that were simulated.

3.1 Materials

To conduct the experiments examining neutron detection in the presence of a large body of water, four ^{3}He detectors (LND Inc Model 252) and two Canberra JSR-14s were utilized. Using two JSRs enabled the signal in each polyethylene block to be kept separate, allowing for a comparison of counts in each of the blocks. The ^{3}He detectors were placed in polyethylene blocks 12.00 in (30.48 cm) long, 6.00 in (15.24 cm) wide, and 2.00 in (5.08 cm) tall. Each polyethylene block could hold two detectors placed 4.00 in (10.16 cm) apart. The signals from both detectors in a polyethylene block were always summed together. The data were collected onto the JSR-14s and then recorded to a Panasonic Toughbook and a Dell desktop computer. A metal rod with a nut and bolt attached (Figure 13) was used to hold the ^{252}Cf source. The rod was marked at 1.00 in (2.54 cm) and at 3.00 in (7.62 cm) intervals up to 24.00 in (60.96 cm). The rod was suspended from a crane and held in place throughout the experiments.

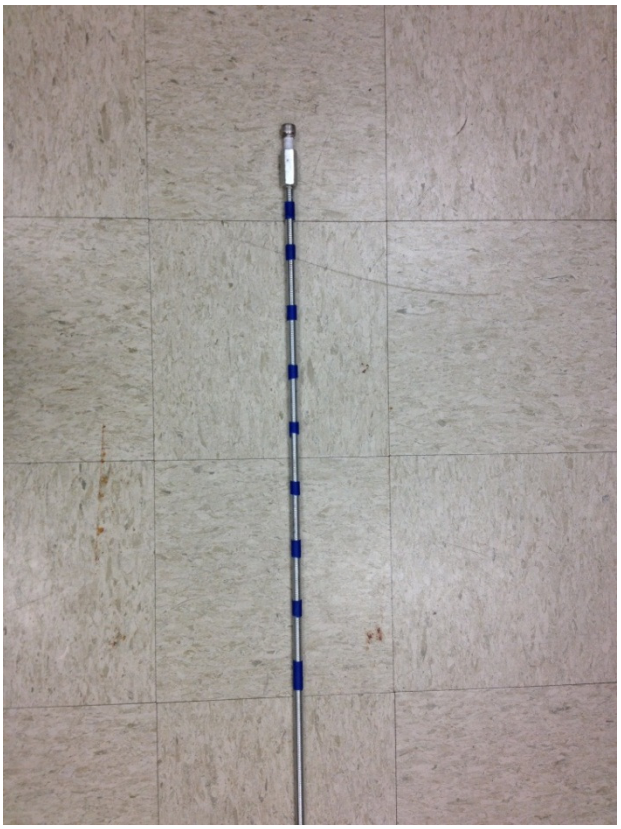

Figure 13. The ^{252}Cf source holder. The source went inside the nut at the top of the figure.

3.2 Location and Setup

The experiments were run at the NSC, which houses a 1 MW Training, Research, Isotopes, General Atomics (TRIGA) reactor. The detectors were placed on a stainless steel bridge spanning a corner of the reactor pool. The bridge was placed 21.00 in (53.34 cm) above the surface of the water. Tests were conducted in the morning before reactor startup and after the reactor had been shut off throughout the night in order to minimize the neutron background. Background counts were initially taken with four detectors parallel to the surface of the water (Figure 14). The cadmium sheet was placed between the polyethylene blocks for the background measurements. Five 10-second measurements were recorded for each pair of detectors. The number of measurements and the count rate time were selected such that random

fluctuations in neutron emission were averaged out. The background count rate was found to be 0.8 ± 0.3 cps. For each subsequent measurement, five 10-second counts were taken.

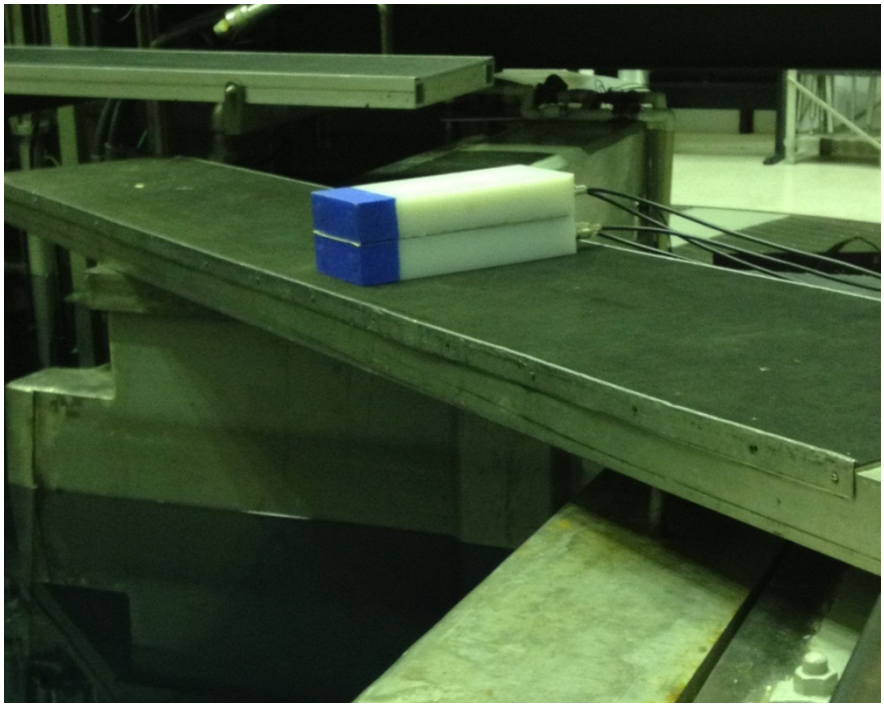

Figure 14. The 4-detector parallel configuration on the bridge over the NSC pool.

3.3 Configurations

Each of the five different configurations from the simulations were used for the experiment. The source was initially placed 1.00 in (2.54 cm) below the surface of the water and all configurations were tested both with and without the cadmium sheet. Initially, the four-detector configuration parallel to the surface of the water with a cadmium sheet between the polyethylene blocks was used (Figure 14). Following that, the two 2-detector parallel configurations were tested. Once the parallel detector configurations were tested, the two

perpendicular configurations were tested, starting with the 4-detector configuration. Figure 15 shows the 4-detector perpendicular configuration being tested with the source above the detectors.

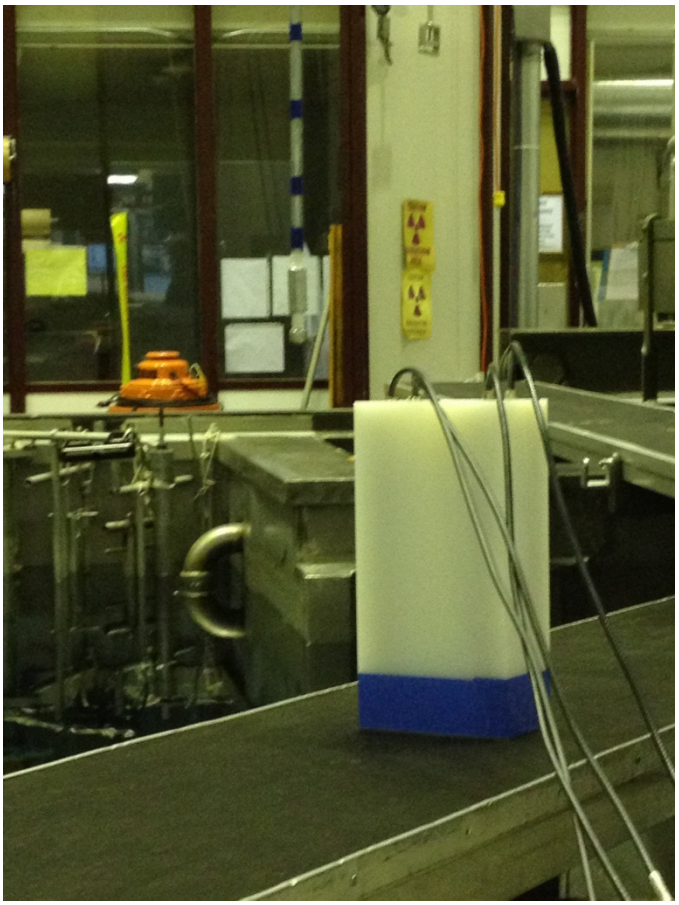

Figure 15. The 4-detector perpendicular configuration. The rod with the source can be seen suspended above the detectors.

3.4 Depths

As with the simulations, both four-detector configurations, one with detectors parallel and the other with detectors perpendicular to the surface of the water, were used to measure a neutron source at set depths below the surface. The cadmium sheet was placed between polyethylene blocks for all tests. The source was positioned at 3.00 in (7.62 cm) intervals below

the surface of the pool and counts were recorded. The final depth tested was 21.00 in (53.34 cm) below the surface. Figure 16 shows the 4-detector parallel configuration with the source in place.

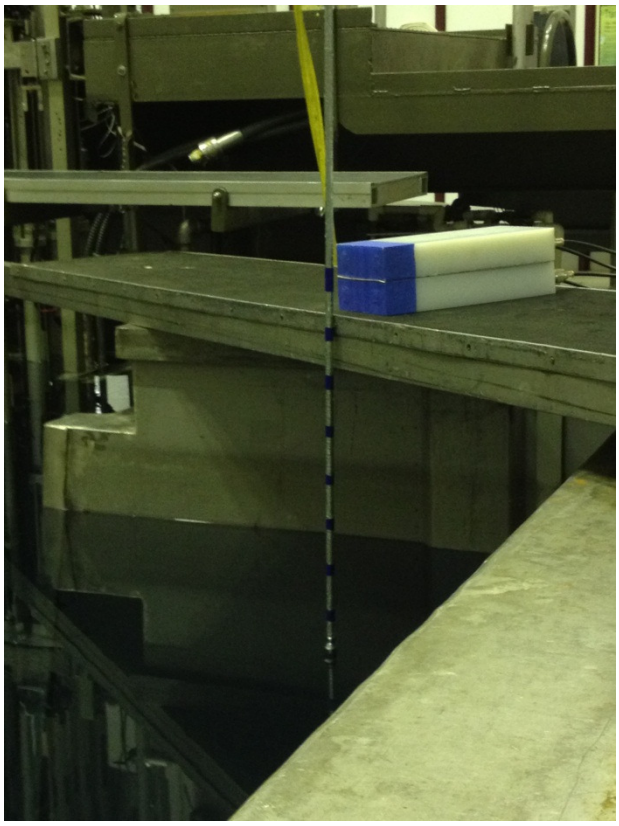

Figure 16. The 4-detector parallel configuration with the source 2.54 cm below the surface.

4. EXPERIMENTAL RESULTS AND DISCUSSION

The following section discusses the results of the experimental measurements taken at the NSC in November 2012 and compares them to the simulations of the same geometry using MCNP. This section will discuss the different detector configurations tested as well as the maximum depth a source below the surface of the water can be detected.

4.1 Background Neutron Count

Experimental measurements of the background count rate at the NSC resulted in a count rate of 0.8±0.3 cps. The background simulation from MCNP resulted in a background count of 0.7±0.2 cps around the detectors, which is in close agreement with the measured values. The MCNP-produced background count rates was expected to be on the order of magnitude of 1 cps, which has been observed by numerous experiments [10] [22] [23].

4.2 Configurations Results

Figure 17 depicts all configurations that were tested in the experiments and simulations. Each configuration is labeled as the way it will be referred to throughout the results. Table II compares the results of MCNP simulations to experimental measurements of a ^{252}Cf source placed 1.00 in (2.54 cm) below the surface of water, with detectors 21.00 in (53.34 cm) above the surface. The uncertainties listed in Table II are all 1-σ standard deviations.

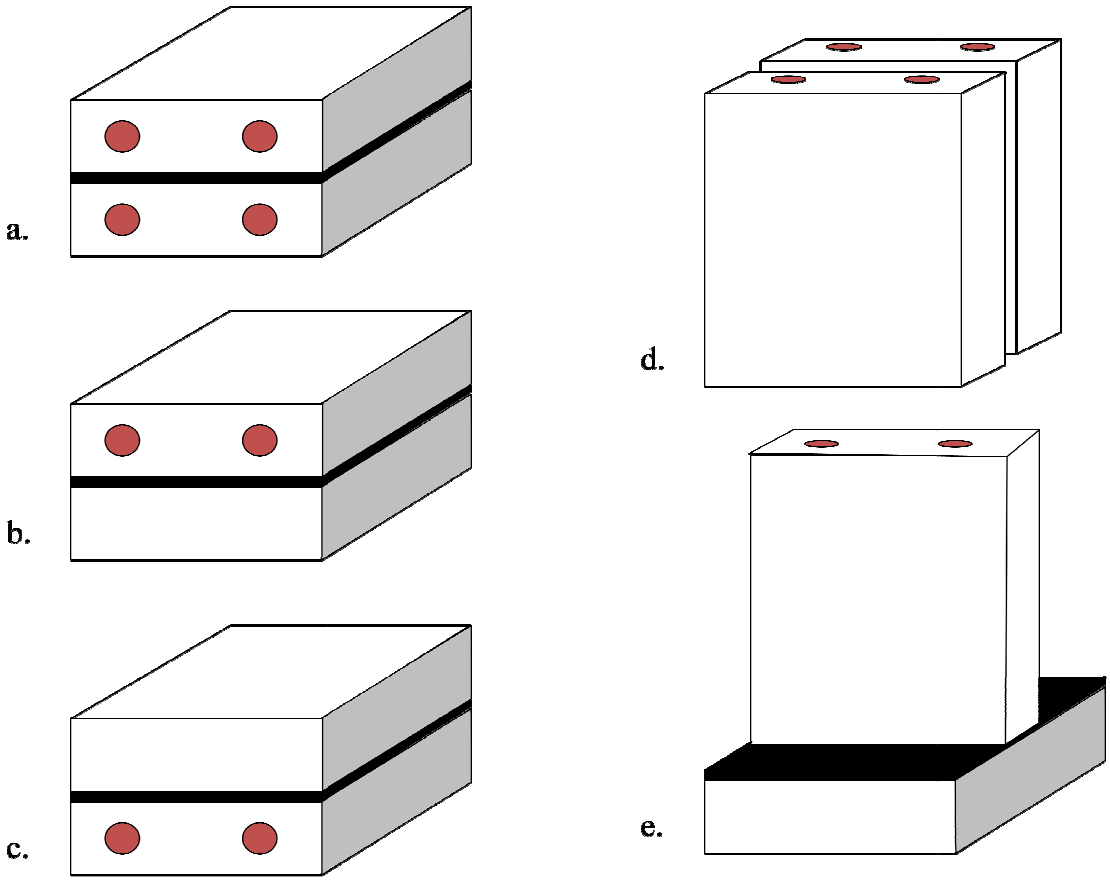

Figure 17. All configurations used in the experiment and simulation. 17a. 4-detector parallel configuration. 17b. 2 parallel detectors on top. 17c. 2 parallel detectors on bottom. 17d. 4-detector perpendicular configuration. 17e. 2-detector perpendicular configuration.

Table II. Detector response to a source located directly below the detectors.

Experimental Configuration		Simulation count rate cps	Experiment count rate cps
4 parallel detectors with cadmium	upper	61.3 ± 0.5	47 ± 3
	lower	462 ± 1	269 ± 7
4 parallel detectors without cadmium	upper	122.3 ± 0.6	84 ± 8
	lower	511 ± 1	316 ± 4
2 parallel detectors on top with cadmium		51 ± 1	48 ± 3
2 parallel detectors on top without cadmium		132 ± 1	96 ± 5
2 parallel detectors on bottom with cadmium		463 ± 2	237 ± 4
2 parallel detectors on bottom without cadmium		526 ± 2	272 ± 3
4 perpendicular detectors with cadmium	left	55.7 ± 0.4	61 ± 3
	right	54.9 ± 0.4	61 ± 6
4 perpendicular detectors without cadmium	left	76.6 ± 0.5	86 ± 5
	right	76.1 ± 0.5	76 ± 5
2 perpendicular detectors with cadmium		15.7 ± 0.2	30 ± 2
2 perpendicular detectors without cadmium		23.7 ± 0.3	38 ± 2

As can be seen, for all parallel configurations, MCNP predicted higher count rates than was measured. For perpendicular detectors, the experimental count rates were higher than the MCNP predictions. This suggests a systematic bias in the MCNP simulations which may be due to neglecting the inactive area in the detector tubes. A ratio of the calculated to experimental values (C/E) was taken and plotted for each detector configuration, shown in Figure 18 and shows this bias. For all configurations, both in simulation and experiment, configurations without a cadmium sheet recorded higher neutron counts. It was expected that count rates would be higher in the simulations because they do not take into account everything in a physical system which could interfere with the count rate and reduce efficiency.

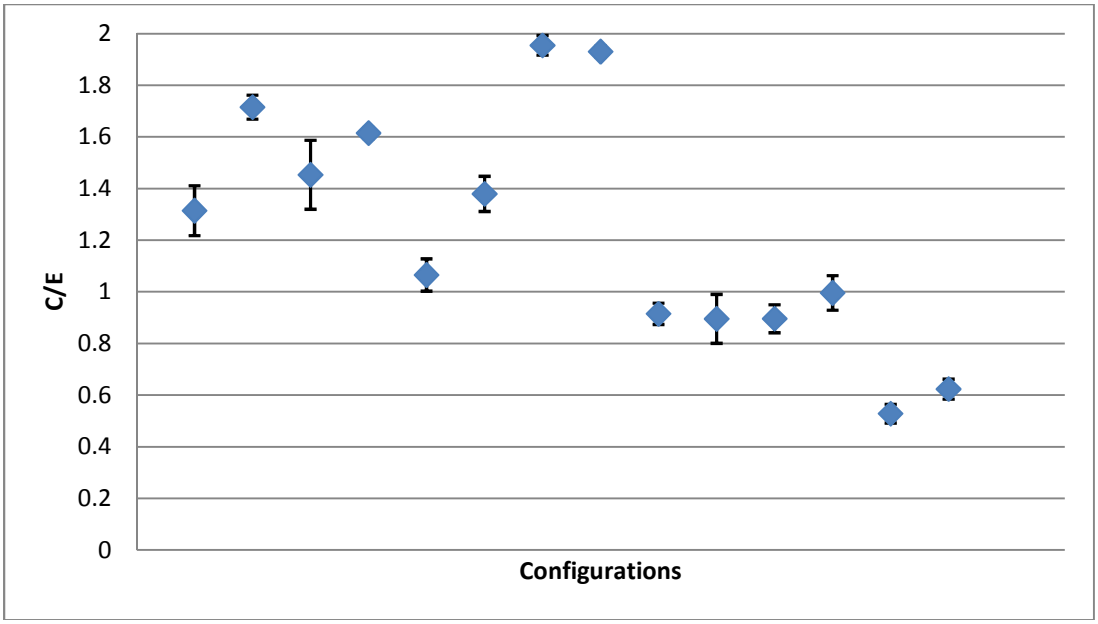

Figure 18. C/E plot comparing experimental and simulated results for a source directly below the detectors. The eight data points to the left are from the parallel configurations while the six data points to the right are from the perpendicular configurations.

The 4-detector configurations were tested to provide some sense of the location of a neutron source. The parallel configuration was intended to provide information on the height of the source, while the perpendicular configuration was designed to provide information on the x/y position of a source. To measure this, the ratio of counts in the lower detectors to the counts in the upper detectors was calculated. For the experimental configuration with cadmium, this ratio was 5.77, while without cadmium it was 3.76. For the MCNP simulations, the ratio was 7.53 for the configuration with cadmium and 4.18 for the configuration without. It was expected the ratio of counts would decrease without the cadmium sheet in place to absorb thermal neutrons.

In comparing the 4-detector parallel configuration with the two 2-detector configurations, similar count rates were observed. Experimentally, the counts for the top detectors, with cadmium, were statistically the same and within one standard deviation, while the counts for the top detectors, without cadmium, were within 2σ. Count rates were expected to be similar between these configurations because the detectors were in the same locations as in the

4-detector assembly. The presence or absence of other detectors should not significantly impact the count rates in the present detectors. MCNP results were statistically significantly different between the top detectors of the 4-detector configuration and the 2-detector configuration. In both cases, the detectors in the 4-detector configuration recorded slightly higher counts.

Comparing the bottom detectors of all parallel configurations yielded similar results. Experimentally, with cadmium, the bottom detectors yielded statistically different results. The 4-detector configuration produced a higher count rate of 269 ± 7 cps while the 2-detector configuration resulted in a count rate of 237 ± 4 cps. Without cadmium, both count rates increased, to 316 ± 4 cps for the 4-detector configuration and 272 ± 3 cps for the 2-detector configuration. MCNP results for the lower configurations with cadmium were within 1σ. Without cadmium, the 2-detector configuration recorded 526 ± 2 cps compared with 511 ± 1 cps for the 4-detector configuration.

Count rates for the parallel configurations were higher than count rates for the perpendicular configurations. This is likely because for the parallel configurations, a greater detector volume was closer to the source, while for the perpendicular configurations, the distance from the source to the detector was a gradient, with only a relatively small detector volume close to the source. Additionally, there is a dead zone at the head of the detector; neutrons entering this region of the detector are not registered as counts. This dead zone was directly above the source for the perpendicular detectors. For the perpendicular 4-detector experimental configuration, count rates of 61 ± 3 cps and 61 ± 6 cps were recorded in the left and right detectors, respectively, compared with a count rate of 269 ± 7 cps for the bottom detectors of the parallel 4-detector configuration. The left and right detectors recorded count rates that were within 1σ of each other for both the experimental and simulated results. This was expected, as the source was equidistant from both the left and right detectors. The MCNP results for the

perpendicular configuration were 55.7 ± 0.4 cps and 54.9 ± 0.4 cps. Without cadmium, count rates once again increased for both the experimental and simulation results. For the experimental configuration, count rates of 86 ± 5 and 76 ± 5 cps were observed, which were within 2σ. Count rates of 76.6 ± 0.5 and 76.1 ± 0.5 cps were recorded in MCNP; within 1σ. The 2-detector perpendicular configuration detected the fewest neutrons in both the simulation and the experiment. Experimentally, count rates of 30 ± 2 and 38 ± 2 cps were recorded with and without cadmium, respectively, almost half the counts recorded by the 4-detector perpendicular configuration. This configuration could have fared poorly based on the location of the moderating polyethylene. This is because all other configurations have both polyethylene blocks parallel to the detectors, so neutrons that scattered out of one polyethylene block had a chance of scattering into the adjacent block and being detected. Only in this configuration was a polyethylene block perpendicular to the detectors. Therefore, neutrons moderated in this block were unlikely to scatter into the polyethylene block with the detectors.

The source was placed at a second location: 1.00 in (2.54 cm) below the surface of the water and directly to the right side of the detectors. Table III compares the simulation and measured results. The C/E plot for the calculated to experimental ratio is shown in Figure 19 and exhibits the same bias as was observed with the source placed directly below the detectors. Higher counts were recorded in the simulations with the detectors in the parallel configurations, while higher counts were recorded experimentally with the detectors in the perpendicular configurations.

Table III. Comparison of simulation and experimental results for a source below and to the right side of the detectors.

Experimental Configuration		Simulation count rate cps	Experiment count rate cps
4 parallel detectors with cadmium	upper	61.3 ± 0.5	59 ± 3
	lower	441 ± 1	360 ± 12
4 parallel detectors without cadmium	upper	119.6 ± 0.6	107 ± 6
	lower	489 ± 1	424 ± 6
2 parallel detectors on top with cadmium		51.2 ± 1	58 ± 1
2 parallel detectors on top without cadmium		128 ± 1	125 ± 4
2 parallel detectors on bottom with cadmium		443 ± 2	359 ± 9
2 parallel detectors on bottom without cadmium		504 ± 2	412 ± 12
4 perpendicular detectors with cadmium	left	51.5 ± 0.4	61 ± 3
	right	63.1 ± 0.5	91 ± 3
4 perpendicular detectors without cadmium	left	73.3 ± 0.5	78 ± 6
	right	83.4 ± 0.5	118 ± 3
2 perpendicular detectors with cadmium		17.5 ± 0.2	38 ± 4
2 perpendicular detectors without cadmium		25.5 ± 0.3	48 ± 4

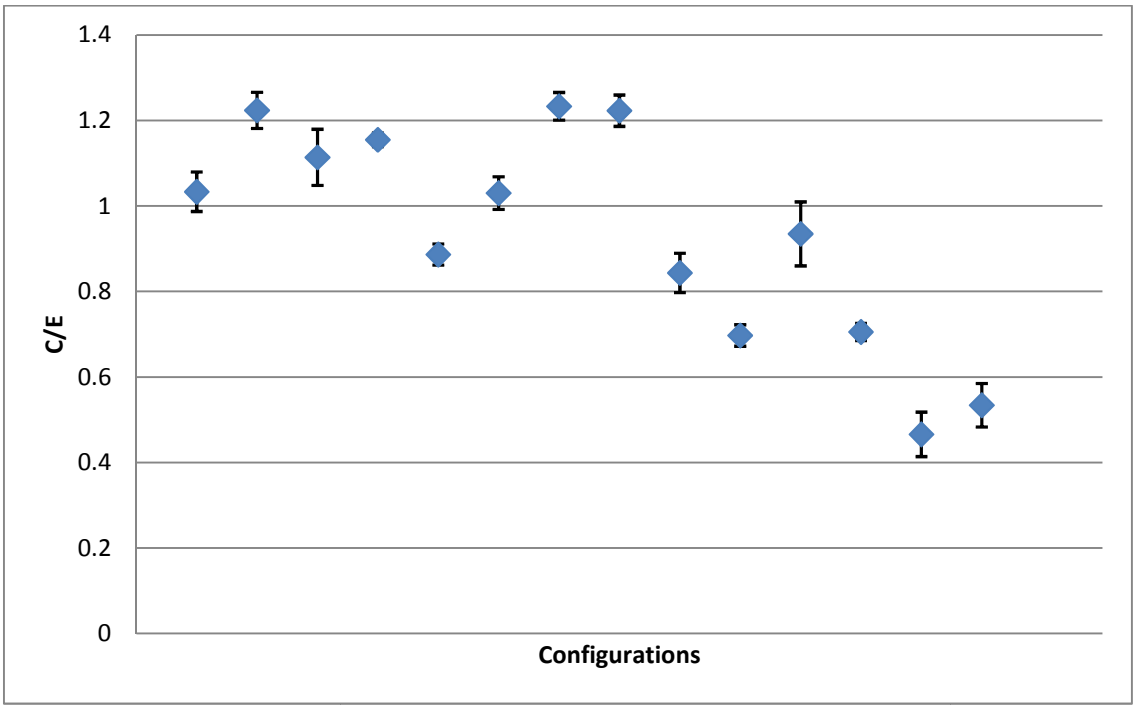

Figure 19. Calculated to experimental ratio for a source placed below and to the side of the detectors. The eight data points to the left are from the parallel configurations while the six data points to the right are from the perpendicular configurations.

Similar trends were noticed compared to a source placed directly below the detectors. Once again, comparing the ratio of counts in the lower and upper detectors of the 4-detector parallel configuration, the ratio was 6.10 for the experimental setup with a cadmium sheet and 3.95 without a cadmium sheet. This was similar to the ratio of 7.23 from the MCNP results with cadmium and 4.09 without a cadmium sheet.

While the count rates for the parallel detectors were similar to those for a source directly below the detectors, the count rates in the perpendicular detectors changed. The source was placed at the same depth below the surface of the water. In the parallel configurations, detector signals were summed for the upper and lower detectors, so a source placed at the same depth but to one side would have similar net count rates as a source directly below the detectors. The increase in the count rate in the detector closer to the source would offset the decrease in count rate in the other detector. However, the perpendicular configuration was expected to be sensitive to the lateral location of a source. The detectors on the right predictably detected more counts than the detectors on the left. Experimentally, there was little difference in the ratio of the counts of the left and right detectors with and without cadmium. With cadmium, the ratio was 1.47, while it was 1.51 without the cadmium sheet. These ratios in MCNP were 1.24 for the configuration with cadmium and 1.14 without cadmium. A large difference in ratios was not expected since the cadmium sheet was largely not between the source and the detectors. Count rates were expected to be higher in the right detectors because the source was closer to these detectors; this was observed. With only two perpendicular detectors, the counts recorded were once again the lowest of any configuration. A marginal increase in count rate in the 2-detector perpendicular configuration was observed in both the experiment and in the simulations when the source was below and to the side of the detectors rather than directly below the detectors.

This is likely because the source was no longer located directly in line with the dead zone in the detectors, allowing for more neutrons that entered the detector volume to be detected.

Table IV shows the results from placing a source above and to the right of the detectors. The source was 11.00 in (27.94 cm) above the top polyethylene block of the 4-detector parallel configuration. Figure 20 shows a plot of the calculated to experimental ratio for this source position.

Table IV. Experimental and simulation results for a source placed above and to the right of the detector configurations.

Experimental Configuration		Simulation count rate s^{-1}	Experiment count rate s^{-1}
4 parallel detectors with cadmium	upper	293 ± 1	215 ± 9
	lower	194.2 ± 0.8	202 ± 1
4 parallel detectors without cadmium	upper	395 ± 1	305 ± 7
	lower	304 ± 1	324 ± 7
2 parallel detectors on top with cadmium		298 ± 3	217 ± 6
2 parallel detectors on top without cadmium		434 ± 3	315 ± 9
2 parallel detectors on bottom with cadmium		185 ± 2	215 ± 6
2 parallel detectors on bottom without cadmium		340 ± 2	341 ± 6
4 perpendicular detectors with cadmium	left	232.9 ± 0.9	137 ± 3
	right	300 ± 1	195 ± 4
4 perpendicular detectors without cadmium	left	354 ± 1	200 ± 2
	right	412 ± 1	282 ± 10
2 perpendicular detectors with cadmium		396 ± 3	184 ± 6
2 perpendicular detectors without cadmium		401 ± 3	192 ± 8

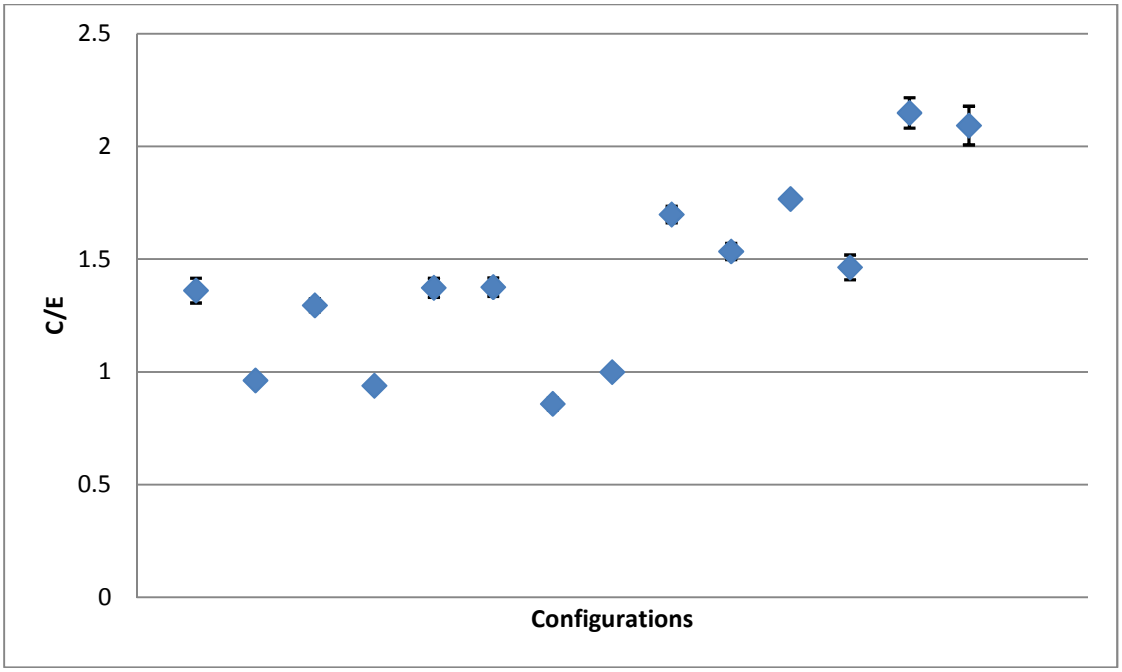

Figure 20. Calculated to experimental ratio for a source placed above and to the side of the detectors. The eight data points to the left are from the parallel configurations while the six data points to the right are from the perpendicular configurations.

For most experimental and simulation results, count rates increased over the two previous source locations. This is due in part to the decreased distance between the source and the detectors. Additionally, the source was not placed in water. Fewer neutrons were moderated and absorbed by the surrounding medium prior to reaching the polyethylene blocks. Count rates did not increase for the lower detectors in the parallel configurations, which were closer to the sources below the water and further from sources placed above the detectors in the air. Additionally, when the source was placed below the detectors, there was also no cadmium shielding between the lower detectors and the source, while there was shielding present when the source was moved above the detectors.

For the 4-detector parallel configuration with cadmium, count rates in the upper detectors were within 2σ of the lower detectors. Without cadmium, the lower detectors detected higher counts, and count rates increased by about 100 cps for both upper and lower detectors.

This is likely because the polyethylene blocks used in the experiment under-moderate neutrons coming to the detectors. Neutrons entering the top polyethylene block were likely still too fast to be detected, and the additional lower polyethylene block moderated them to speeds where they could be detected by the lower detectors. This trend was not noticed when the source was placed below the waterline because the water moderated the neutrons prior to them reaching the detectors. This trend was not observed in the simulations; while count rates did rise around 100 cps without cadmium in MCNP, the upper detectors always recorded a higher count rate than the lower detectors. Count rates in the 2-detector configurations compared to the 4-detector configurations were similar to each other. Count rates in the upper detectors were within 1σ with cadmium and within 2σ without cadmium. Count rates in the lower detectors for the 2-detector configuration were marginally higher than the lower detectors of the 4-detector configuration. Again, the similarities in count rates were expected since the geometry was unchanged.

The perpendicular detectors still recorded lower count rates than the parallel configurations, but there was a difference between the counts recorded in the left and right detectors. With cadmium, the experimental ratio of counts in the left and right detectors was 1.42, while it was 1.40 without. In MCNP, this ratio was 1.29 with cadmium between the detectors and 1.16 without cadmium. While not as great as the ratio between upper and lower detector count rates for sources below the detectors, this difference in count rates could still provide directional detection capabilities. The 2-detector perpendicular configuration once again recorded the fewest counts. The count rates with and without cadmium for this configuration were within 2σ of each other. Compared to the right detectors in the 4-detector perpendicular configuration, similar count rates were observed with cadmium, but without cadmium, the 100 cps increase in the 4-detector configuration was not observed in the 2-detector configuration.

4.3 Depth Measurements and Results

MCNP simulations were run with both of the four-detector configurations using a point source at increasing depths below the surface of the water. An alarm threshold of 3σ above the background was used. Once count rates dropped below this threshold of 1.4 cps, the source could no longer be distinguished from the background. Both configurations included a cadmium sheet between the polyethylene blocks. Figure 21 shows the counts recorded for the detectors in the parallel configuration. The counts for the two bottom detectors were summed together, as were the counts in the two upper detectors. As expected, the lower detectors detected more neutrons than the upper detectors due to the cadmium shielding. For comparison, Figure 22 shows the counts recorded for the MCNP simulations.

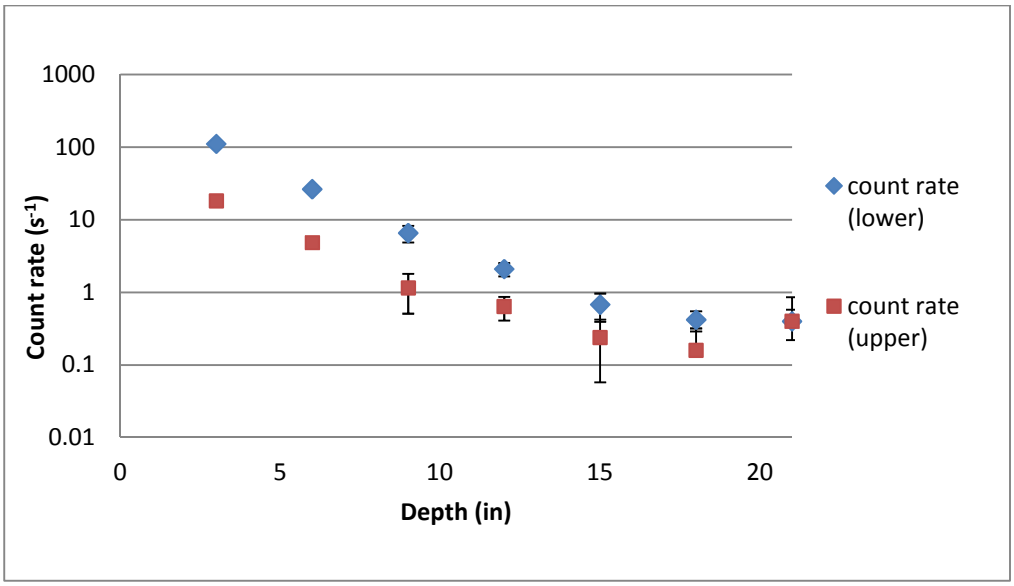

Figure 21. Results for the depth experiments using parallel detectors at the NSC pool.

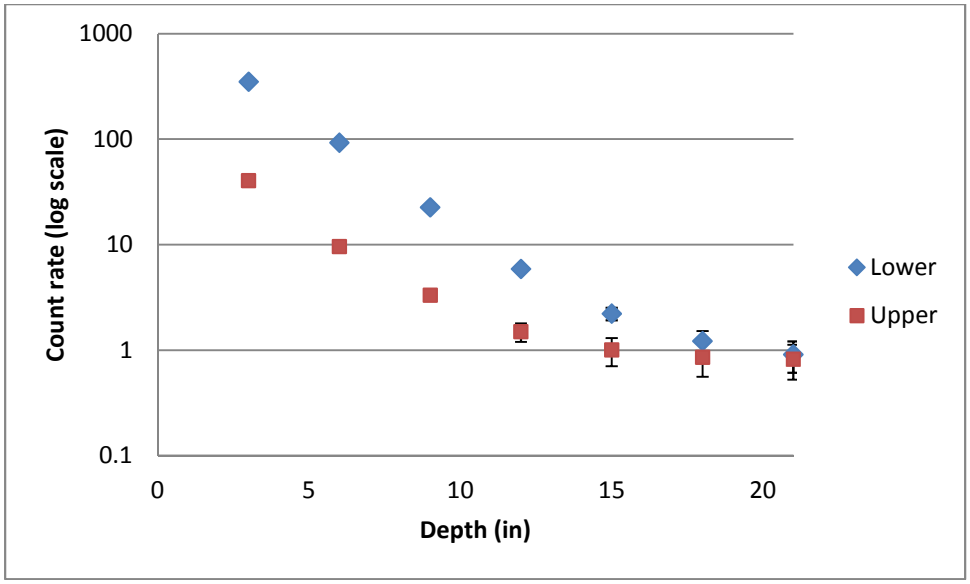

Figure 22. Results for the depth simulations using parallel detectors.

From the experiment, the ^{252}Cf source could be placed to a maximum depth of 12.00 in (30.48 cm) before the counts dropped to background levels and the source could not be distinguished from the neutron background. The simulations predicted the source could be detected above background by both upper and lower detectors down to a depth of 15.00 in (38.10 cm); at a depth of 18.00 in (45.72 cm), only the lower detectors would be above background. Count rates in the simulations were three times higher than the experimental count rates in the lower detectors and twice as high as count rates in the upper detectors.

Table V shows the ratio of the counts in the lower detectors to those in the upper detectors. The ratio decreases with increasing depth, initially beginning with a ratio of 6.1 ± 0.6 obtained in the experiment, compared with a ratio of 8.7 ± 0.1 from the MCNP simulation. There was a greater ratio in the simulation than there was experimentally, likely as a result of the overall higher count rates. In the simulations, the count rates in the lower detectors were higher than the experimental results by a greater fraction than for the upper detectors, contributing to a

higher ratio. As the depth of the source increased and count rates dropped in both detectors, the ratio generally decreased and approached one when counts could no longer be detected above background.

Table V. Comparison of the ratio of counts in the lower and upper detectors as a function of source depth.

Depth (in)	Ratio of counts (simulation)	Ratio of counts (experimental)
3	8.7 ± 0.1	6.1 ± 0.6
6	9.6 ± 0.4	5 ± 1
9	6.8 ± 0.7	6 ± 3
12	3.9 ± 0.8	3 ± 1
15	2.2 ± 0.7	3 ± 2
18	1.4 ± 0.6	3 ± 3
21	1.1 ± 0.5	1 ± 1

The ratio of counts in the lower and upper detectors in the parallel configuration was significant for sources below the waterline, but it was not apparent for sources above the waterline. Using ratios, the detectors would be unable to determine whether a source was 21.00 in (53.34 cm) below the water, where counts are very low, or if a source were in the air above the detectors. However, count rates were much higher for sources in the air than for sources deep in water. By using a combination of both count rates and detector response ratios, the detectors would be better able to determine the location of a source of known strength. Nevertheless, the detectors would still be unable to determine the difference between a weak source above the waterline and a strong source deep below the waterline. This can be mitigated by adding perpendicular detectors, which could provide the lateral location of the source.

At low depths, the perpendicular detectors recorded fewer counts than the parallel detectors, but the maximum depth the detectors could detect sources was not much different

from the parallel detectors. Additionally, the count rates in the perpendicular detectors were the same, within 2σ. This was expected, as the source was equidistant from both the left and right detectors. Figure 23 shows the experimental results, while Figure 24 shows the simulation results. Experimentally, the source could be detected above background only to a depth of 9.00 in (22.86 cm). The simulations predicted the source could be detected down to 12.00 in (30.48 cm). Also of note in the simulations was the similarity in count rates between the perpendicular detectors and the upper detectors of the parallel configuration. The difference in count rates was less than 1 cps for a source at a depth greater than 3.00 in (7.62 cm). Experimentally, count rates between the perpendicular detectors and the upper parallel detectors were also similar, but not as close as the simulation results. The upper parallel detectors recorded fewer counts than the perpendicular detectors. The more advantageous detector geometry in the parallel configuration was counteracted by the lack of cadmium shielding between the source and detectors for the perpendicular configuration.

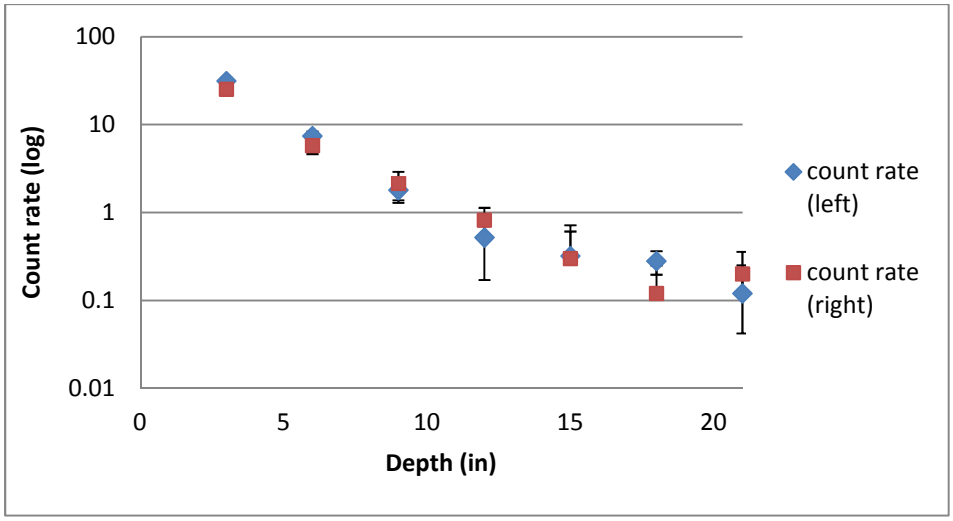

Figure 23. Results for the depth experiments using perpendicular detectors at the NSC pool.

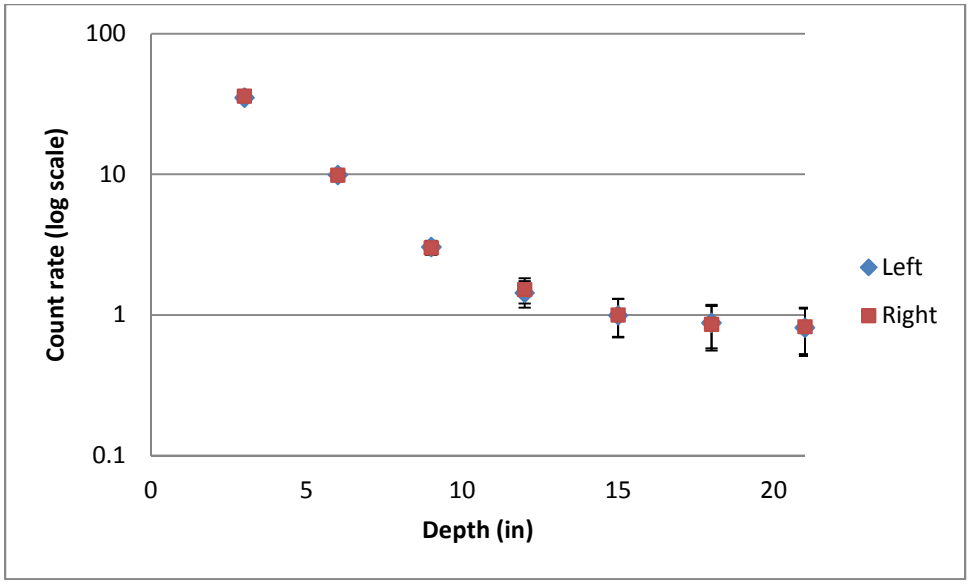

Figure 24. Results simulating perpendicular detector response to sources at increasing depths.

5. ADDITIONAL SIMULATIONS RESULTS AND DISCUSSION

This section details the additional simulations that were run using MCNP. The results for moving sources both below and above the waterline will be discussed. This section will also describe detector response to a source placed in a wave environment.

5.1 Wave Simulations

5.1.1 Detectors Placed Directly Above the Waves

MCNP simulations were run modeling the effect of waves on the detection capabilities with the 4-detector parallel configuration, with a cadmium sheet between the polyethylene blocks. The 4-detector perpendicular configuration was not used for this simulation because it did not perform as well as the parallel detectors in detecting sources under water. Also, comparisons were made between upper and lower detectors; because the source was placed directly beneath the detectors, the perpendicular detectors were expected to record the same counts. A ^{252}Cf source was placed at a constant depth of 3.00 in (7.62 cm) below the surface of a flat plane of water, and cylindrical waves of radius 3.00 in (7.62 cm), 6.00 in (15.24 cm), 9.00 in (22.86 cm), and 12.00 in (30.48 cm) were created. Figure 25 shows the eight locations, numbered 0 through 7, corresponding to eight equally spaced locations in the wave period. The source was placed at each location, and the detector was placed directly above the source. Positions 0 and 4 were where the neutron source was directly between an air and a water cylinder. The source was placed in the air, out of the water, in positions 1 through 3, and the source was under water for positions 5 through 7.

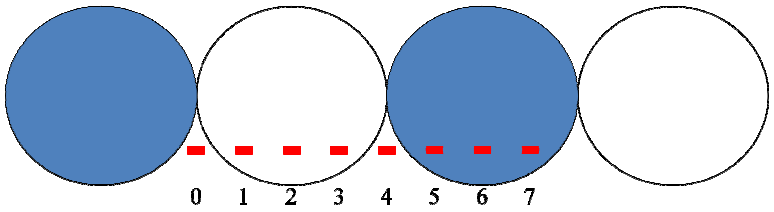

Figure 25. Source and detector locations for the wave simulations.

Figure 26 shows the count rates in the lower detectors with the detectors placed 1.00 in (2.54 cm) above the peak of the waves. The detectors were placed just above each wave to model the situation in which the detectors would be placed on a buoy or some other floating device, the motion of which is dependent on the changing sea state. Count rates were compared to detectors placed at the same height above a flat plane of water. This maintained the same distance between the neutron source and the detectors and provided a basis of comparison for the expected count rates. The count rates above the flat plane of water are represented by the flat lines in the figure. Figure 27 shows the count rates in the upper detectors in the same configuration.

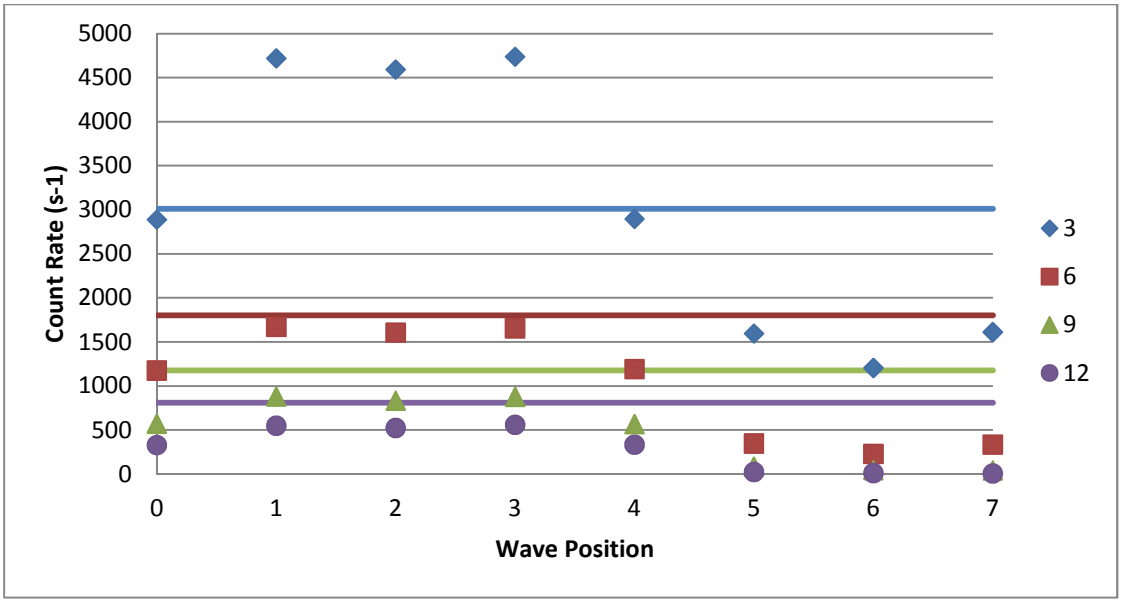

Figure 26. Lower detector count rates for detectors positioned 1.00 in above the peak of the wave.

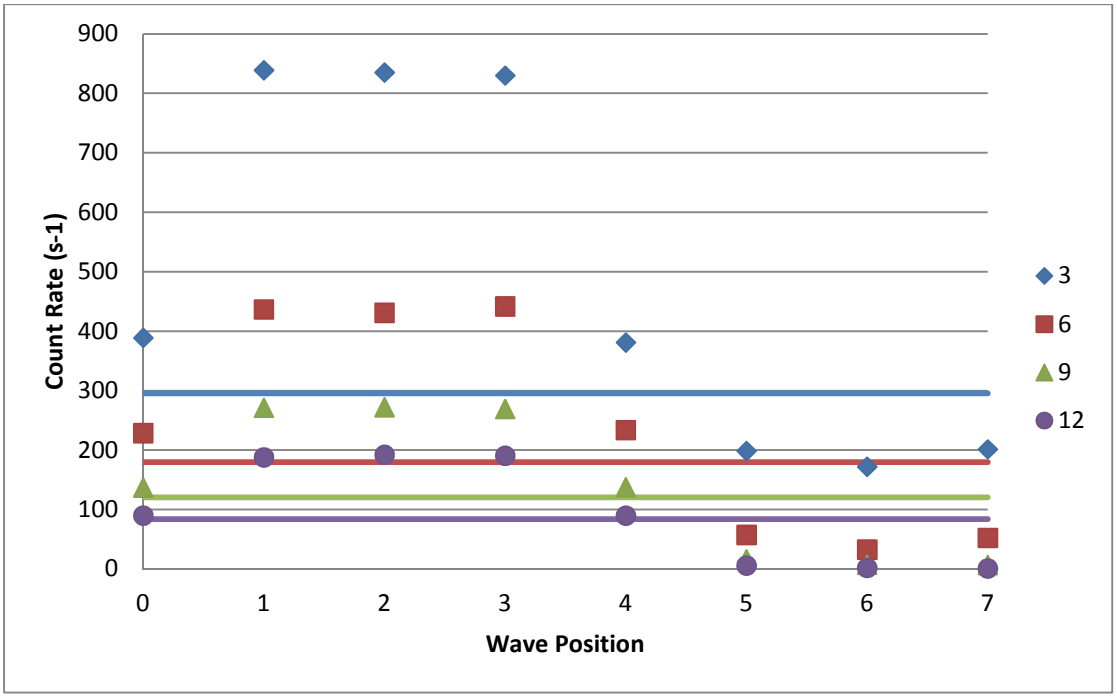

Figure 27. Upper detector count rates for detectors positioned 1.00 in above the peak of the wave.

For the 3.00-in waves, the average count rate for the wave system was greater than the count rate over a flat plane of water for both the lower and upper detectors. For the lower detectors, the average count rate above waves was 3031 ± 4 cps, fluctuating from a high of 4738 ± 12 cps to a low of 1207 ± 6 cps, a factor of 3.93 fewer counts. This fluctuation is due to the waves and not geometry, as the source-to-detector geometry was constant for all simulations. This was greater than the 3009 ± 10 cps in the lower detectors above a flat plane of water. In the lower detectors, only three source positions, the three with the source out of the water and in the air, resulted in higher count rates than for a source above a flat plane of water. In the upper detectors, the count rates fluctuated between 838 ± 5 cps and 172 ± 2 cps, a factor of 4.87. The average count rate above waves, 480 ± 1 cps, was greater than the 295 cps ± 3 above a flat plane. For the upper detectors, there were five source locations with individual count rates higher than the count rate above a flat plane. Only when the source was below the peak of the wave, in positions 5 through 7, were the count rates lower than the count rates above a flat plane.

With 6.00-in waves, the average count rate for the lower detectors of 1027 ± 2 cps was lower than that of the detectors above a flat plane of water, with a count rate of 1802 ± 8 cps. Unlike the 3-in wave system, a source located at any position in the wave period for 6-in waves resulted in lower count rates than if the source had been located under a flat plane of water. The fluctuation in count rate increased from the 3-in wave system. For the lower detectors, the count rates fluctuated by a factor of 7.27; from a low of 230 ± 3 cps to a high of 1672 ± 8 cps. In the upper detectors, similar trends were observed to the 3-in waves. The average count rate in the upper detectors was 239 ± 1 cps, greater than the count rate of 180 ± 2 cps above the flat plane. Again, with the source located at five of the eight points in the wave period, higher count rates were observed in the wave system than for the detectors placed above the flat plane. The

fluctuation in the count rate increased as well, ranging from a low of 33 ± 1 cps to a high of 441 ± 4 cps, a factor of 13.36 different.

Similar trends were observed with 9.00-in waves. The average count rate registered in the lower detectors was 490 ± 1 cps, lower than the 1175 ± 6 cps registered in the lower detectors above a flat plane of water. As count rates decrease with a greater source-to-detector distance, the fluctuation in the count rate increased. The count rate fluctuated by over a factor of 20, from a low of 44 ± 1 cps to a high of 884 ± 5 cps. This variance was even more pronounced in the upper detectors, where the count rates varied by nearly a factor of 40. The upper detectors averaged higher count rates above waves than above a flat plane of water, with count rates of 140 ± 1 cps and 121 ± 2 cps, respectively.

These trends were further exhibited when simulations were run with 12.00-in waves. The lower detectors had higher count rates above a flat plane of water than above waves, with count rates of 812 ± 5 cps and 294 ± 1 cps, respectively. The fluctuation in counts during the wave period increased to a factor of 62 as count rates when the source was under the crest of a wave dropped to 9 cps. In the upper detectors, the count rate above waves was still higher than the count rate above a flat plane, but the difference in count rates, 95 ± 1 cps compared to 84 ± 2 cps, was smaller. With a source below the crest of a 12.00-in wave, the upper detectors would be unable to distinguish the source from the neutron background.

Count rates were expected to increase when the source was in the air and not in the water, but the reflection and moderation from the surrounding water decreased the count rates. As the wave size increased, there was an increasing amount of water surrounding the source, even when it was out of the water, likely contributing to the decreasing count rates as the wave size increased. Additionally, as the wave size increased, the distance between the source and detector increased, further decreasing the counts.

As the wave size increases, the difference in the average count rates for the lower detectors compared to detection rates above a flat plane of water increases, indicating the lower detectors are more susceptible to a changing sea state. A ratio of the average count rate above waves to the count rate above flat water was created; this ratio starts close to one with 3.00-in waves and decreases as wave size increases. Increasing moderation by the water, particularly when the source is below the crest of a wave as it is in positions 5-7, results in decreasing count rates in the detectors. The average count rate is decreasing faster than the count rate decreases for a source above a flat plane of water, resulting in a lower ratio.

The opposite trend is apparent in the upper detectors. Here, the drop in count rates is comparable between the count rates above a wave compared to above a flat plane of water. The difference in count rates decreases with increasing wave size, and as a result, the ratio between the count rates approaches one. The count rates in the upper detectors are significantly lower than the count rate in the lower detectors due to the greater distance between source and detector, the presence of more moderation, and the presence of the cadmium sheet to absorb thermal neutrons. The shape of the water, whether a flat plane or a wave, had less of an impact on average count rates in the upper detectors as a result. Table VI shows the ratio of the average count rates above a wave versus the count rates above a flat plane of water for both the lower and upper detectors. A ratio less than one is indicative of higher count rates above a flat plane of water, while ratios greater than one are representative of higher average count rates above waves.

Table VI. Ratio comparing the average count rate above waves versus a flat plane of water for both lower and upper detectors directly above the waves.

Wave Height (in)	Lower Detectors	Upper Detectors
3.00	1.01	1.63
6.00	0.57	1.33
9.00	0.42	1.16
12.00	0.36	1.13

Similar to the configuration experiments, the ratio of counts in the lower and upper detectors was calculated for each position in the wave. Figure 28 compares these ratios for each wave size. As can be seen, not only do the count rates fluctuate depending on the source position in the wave, but the ratio fluctuates as well. Count rates in the upper detectors fluctuated more than count rates in the lower detectors. This ratio is lowest when the source is positioned in air, in positions 1 through 3, when count rates are the highest. This matches with the configurations experiments, where the ratio between count rates was greater when the source was located under water and lower when the source was out of the water. The count rate in the upper detectors increases more than the count rate in the lower detectors, resulting in a lower ratio. When the source is positioned in the water, count rates in the upper detectors drop quicker than count rates in the lower detectors; this effect becomes more pronounced as wave size increases. The moderation, both from the polyethylene and the increasing amount of water between the source and the detector, has a greater impact on the detectors with lower count rates.

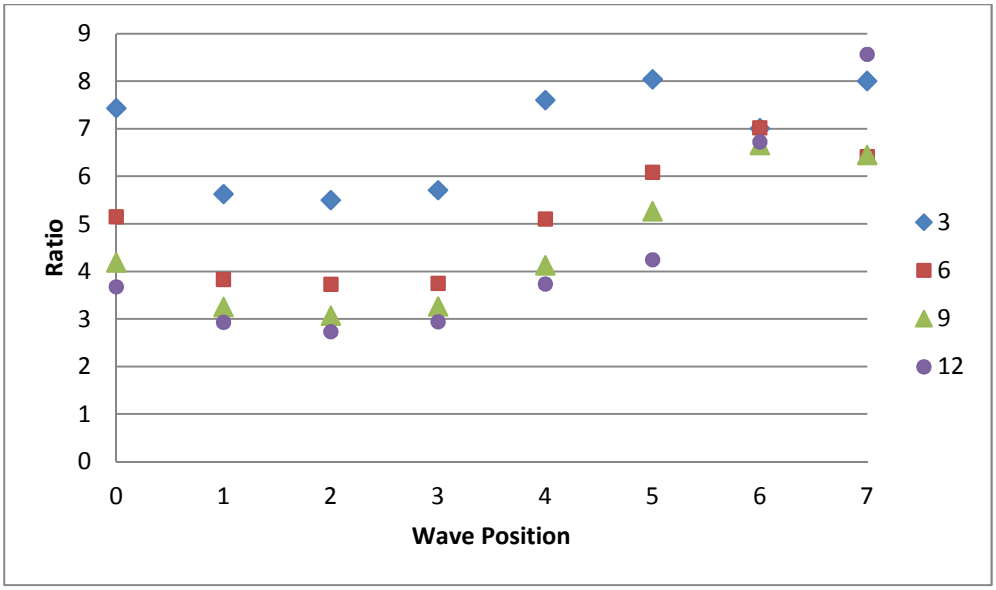

Figure 28. Ratio of counts in lower and upper detectors for each position in the wave period.

5.1.2 Detector Placed High Above the Waves

A second set of simulations were run with the detectors consistently placed 2.00 ft (60.96 cm) above the plane of the water, regardless of wave height. The purpose of these simulations was to model a detector system that would be placed on an object that was stationary compared to the water, such as a bridge or a dock. Again, cylindrical waves of radius 3.00 in, 6.00 in, 9.00 in, and 12.00 in were created and a ^{252}Cf source placed at the same depth as previous simulations at the same eight locations in a wave period. Figure 29 shows the count rates in the lower detectors as compared to a detector above a flat plane of water, while Figure 30 shows the count rates for the upper detectors.

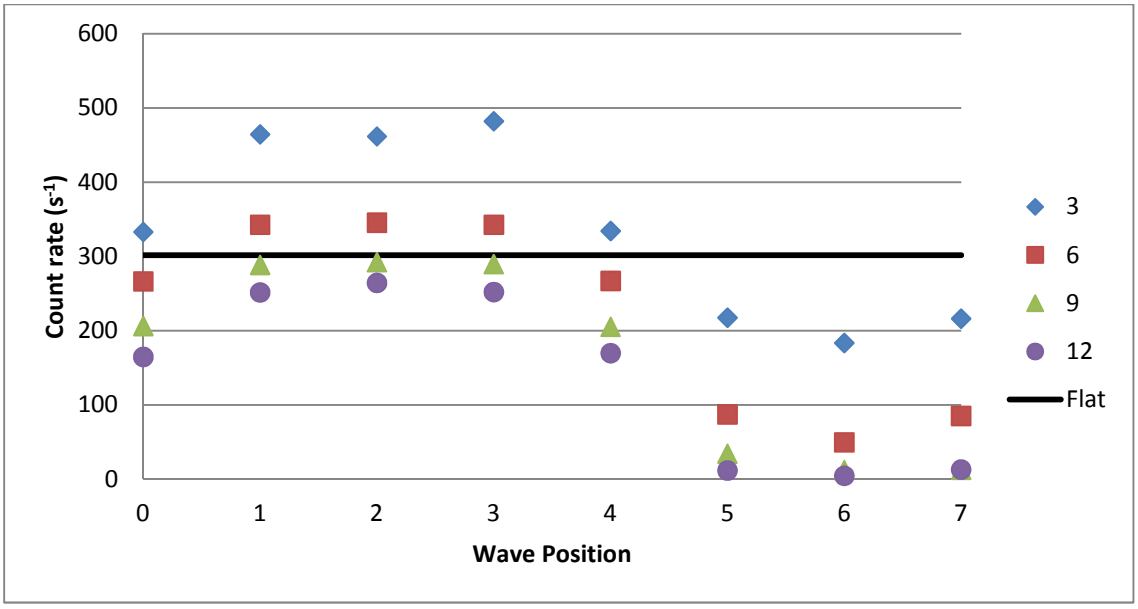

Figure 29. Lower detector count rates for detectors positioned 2.00 ft above the plane of water with varying wave heights.

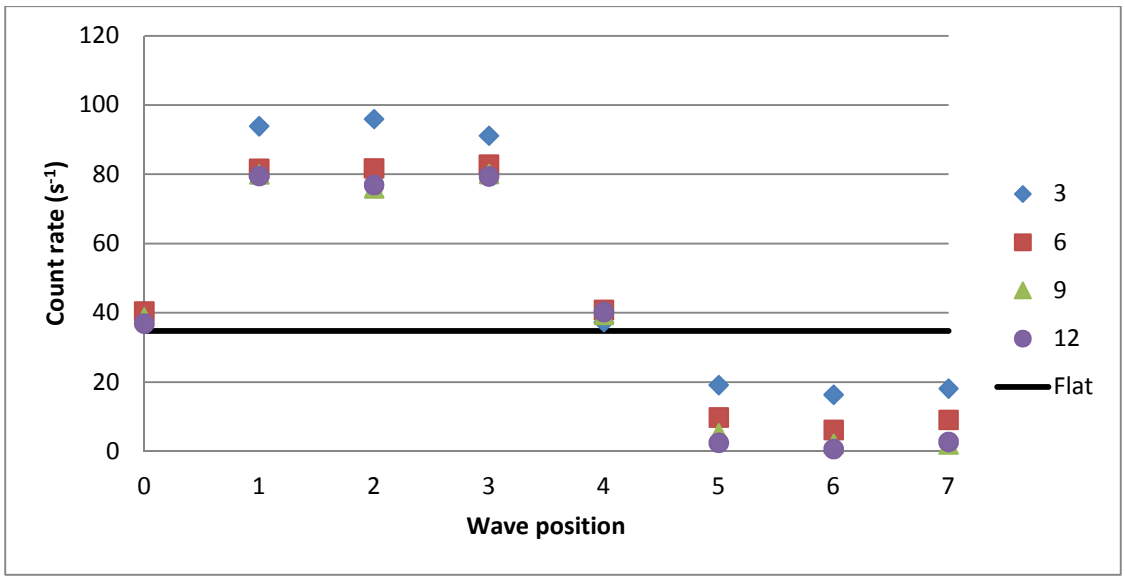

Figure 30. Upper detector count rates for detectors positioned 2.00 ft above a plane of water with varying wave heights.

Similar trends as those observed in the previous wave simulation were exhibited. With 3.00-in waves, both lower and upper detectors recorded higher count rates than the detectors placed above a flat plane of water. Above a plane of water, 302 ± 3 cps were recorded in the lower detectors and 35 ± 1 cps were recorded in the upper detectors. The count rate in the lower detectors was 337 ± 1 cps and 51.1 ± 0.5 cps in the upper detectors. The count rate in the upper detectors was higher above waves of all heights than above a flat plane. This is due to the higher count rates when the source was in positions 1-3, in the air. The count rates above 6.00-in, 9.00-in, and 12.00-in waves were 44.0 ± 0.4 cps, 40.5 ± 0.4 cps, and 39.9 ± 0.4 cps, respectively. The greater distance between source and detectors reduced the total counts in the upper detectors to a rate where the waves made little impact on the average count rate.

Like the previous scenario, the count rate in the lower detector was greater over a flat plane of water than over 6.00-in, 9.00-in, and 12.00-in waves. The average count rate for these wave heights was 223 ± 1 cps, 168 ± 1 cps, and 142 ± 1 cps, respectively. The difference between the average count rates above waves and the count rate above a flat plane of water was lower for the higher detector position. Overall, lower count rates, brought on by the increased distance from the waves, resulted in less difference between the results. The attenuation of neutrons in the air lessened the impact on count rates by the waves. This resulted in ratios closer to one when comparing the count rates between the waves and the flat plane. Table VII displays the ratio of count rates above waves versus above a plane of water.

Table VII. Ratio comparing the average count rate above waves versus a flat plane of water for both lower and upper detectors high above the waves.

Wave Height (in)	Lower Detectors	Upper Detectors
3.00	1.12	1.46
6.00	0.74	1.26
9.00	0.56	1.17
12.00	0.47	1.14

Count rates were close to an order of magnitude lower than when the detectors were directly above the waves. This is due in part to the increased distance between the source and the detector. Count rates drop off as $1/r^2$ as the distance between source and detector increases; doubling the distance should result in a decrease in the count rate by a factor of four. For the 9.00-in waves, the second simulation, with the detectors high above the waves, placed the detectors twice as far from the source as in the initial simulation with the detectors directly above the wave. The average count rates dropped less than expected; The average count rate in the lower detectors dropped by nearly a factor of three, while the count rate in the upper detectors dropped by a factor of 3.4.

5.1.3 Wave Simulations with Source Moving Relative to the Detectors; Detectors Placed Directly Above the Waves

The wave simulations were repeated, but this time, the source was held stationary at position 0 while the detectors were moved to the eight locations. This was done to determine if similar effects were seen when the source was moving relative to the detectors. These simulations were initially run with the detectors placed directly above the peak of the waves.

The source was kept at a depth of 3.00 in below the plane of the water. Figure 31 shows the lower detector response to a moving source while Figure 32 shows the upper detector response.

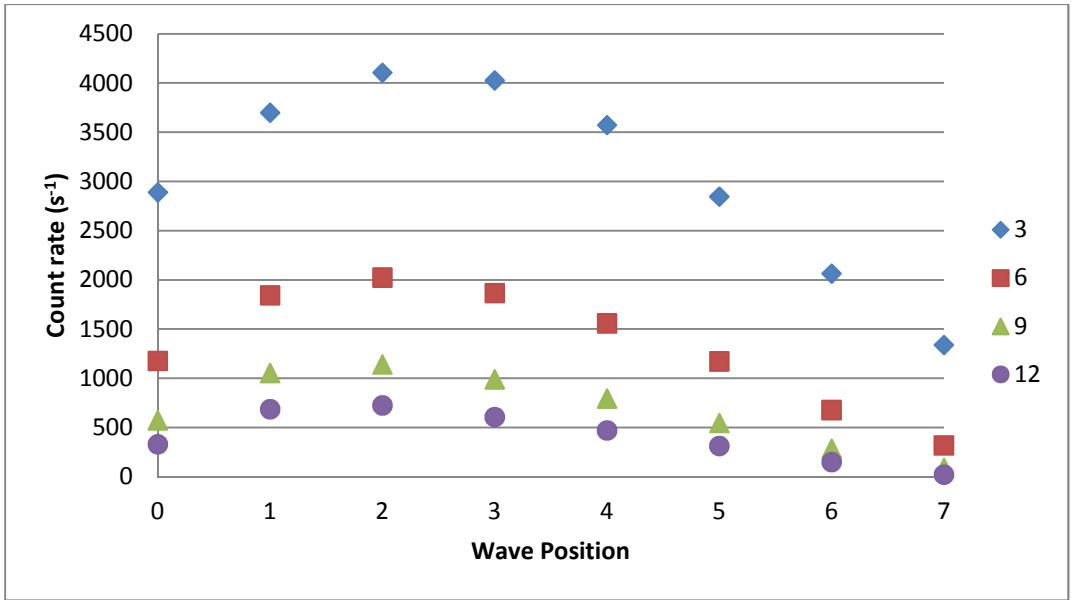

Figure 31. Average count rates in the lower detectors for waves of varying heights.

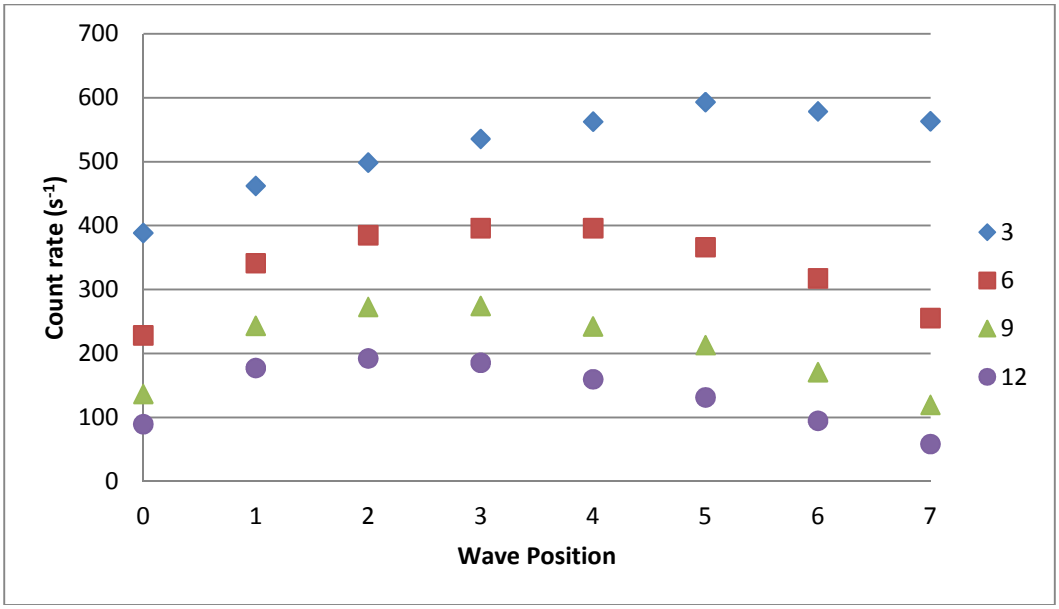

Figure 32. Average count rates in the upper detectors for waves of varying heights.

In these simulations, the source was consistently placed under water, close to the air/water interface (position 0 in Figure 25 on page 41). In the lower detectors, count rates were higher when the detectors were above the trough of a wave, then decreased as the detectors moved over a wave peak. This behavior was consistent for all wave heights, indicating that the source environment, whether water or air, has a greater impact on neutron count rates than source-to-detector distance. As the amount of water decreased between the source and the detectors, count rates increased despite increasing source-to-detector distances. In the upper detectors, count rates above 3.00-in waves increased with increasing source-to-detector distance. For increasing wave heights, count rates followed the same pattern as count rates in the lower detectors; increased count rates were observed when the detectors were above the trough of a wave, and decreased as the detectors moved over the peak of a wave.

5.1.4 Wave Simulations with Source Moving Relative to the Detectors; Detectors Placed High Above the Waves

A moving source was additionally simulated with the detectors in the high position. The source was placed in the same location, position 0, as the previous simulation and the detectors were again 2.00 ft above the water, as in section 5.1.2, and moved to the same eight locations in the wave period. Figure 33 shows the lower detector responses with varying wave heights while Figure 34 shows the upper detector response.

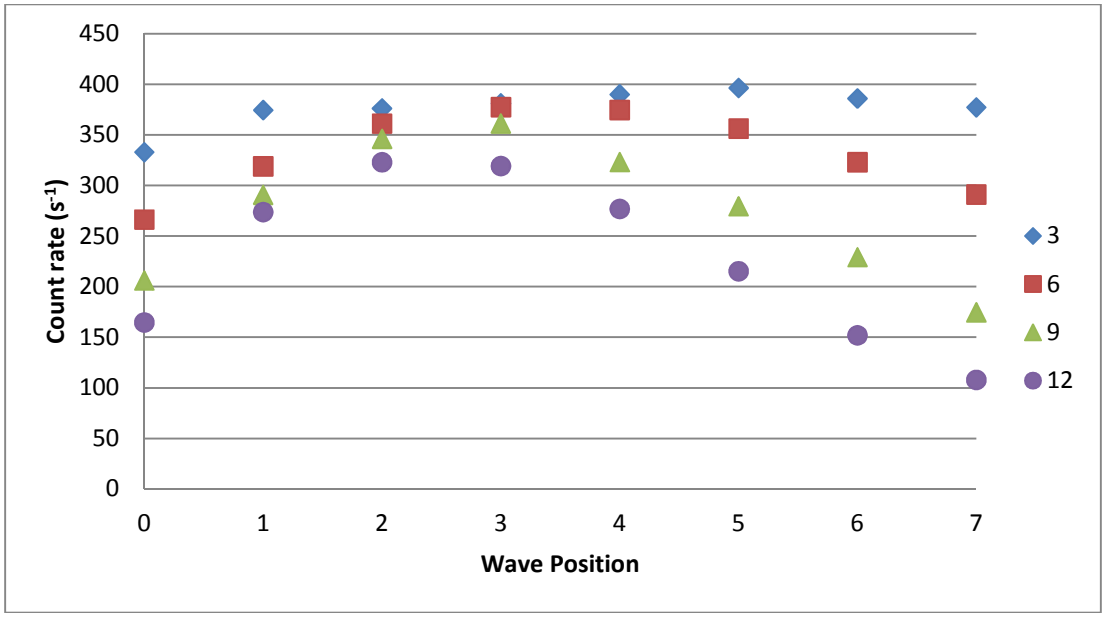

Figure 33. Average count rates in the lower detectors for waves of varying heights with the detectors a constant height above the plane of water.

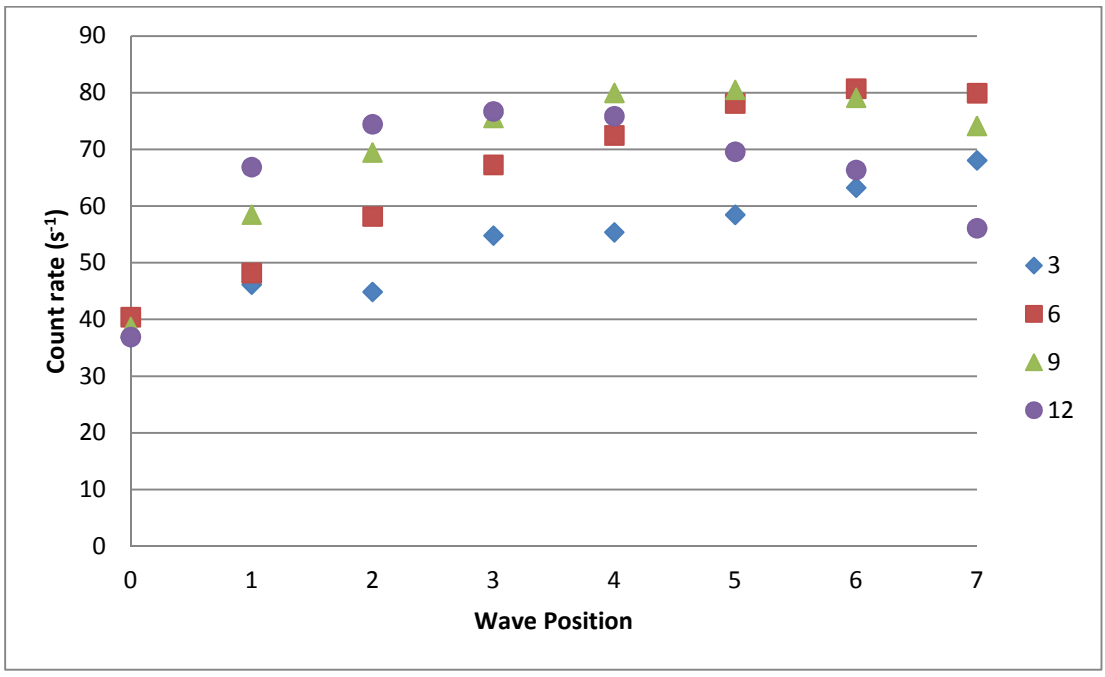

Figure 34. Average count rates in the upper detectors for waves of varying heights with the detectors a constant height above the plane of water.

Similar to the response when the detectors were placed directly above the waves, count rates increased as the detectors were moved over the trough of a wave. Overall count rates were an order of magnitude lower than when the detectors were placed directly over the waves. In the lower detectors, count rates did not drop as precipitously as the distance between the source and detectors increased for 3.00-in and 6.00-in waves compared to when the detectors were placed directly above the waves. This is likely due to the change in distance between the detectors and the source. The distance between source and detector can be imagined as the hypotenuse of a right triangle, shown in Figure 35, where *a* is the height of the detector above the water plus the depth of the source below the water, *b* is the lateral movement of the detector, and *c*, the hypotenuse, is the actual source-to-detector distance. The Pythagorean Theorem in Eq. 6 defines the source-to-detector distance, *c*.

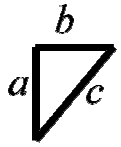

Figure 35. The relationship between the detector position and the distance between source and detector.

$$c = \sqrt{a^2 + b^2} \qquad \text{Eq. 6}$$

With the detectors directly (h_1) above the waves, though, lateral movements of Δx of the detectors significantly increased the distance between the source and the detector. The same lateral movement in detectors placed much higher (h_2) above the waves resulted in less of a change in the actual distance between the source and detector, resulting in less of a decrease in count rate. This difference can be seen in Figure 36.

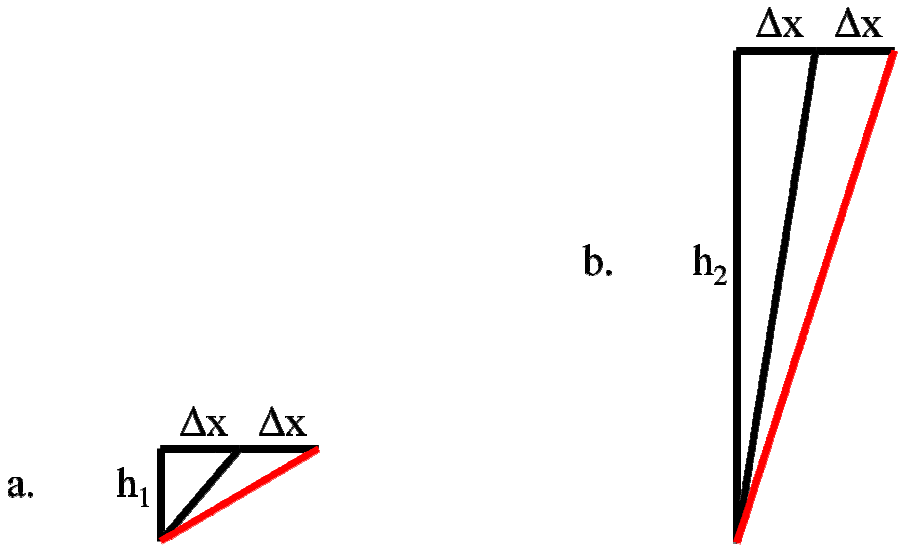

Figure 36. With the detectors close to the waves (36a), changes of detector location by Δx have a greater impact on the source-to-detector distance, shown in red, than when the detectors were high above the waves (36b).

For 3.00-in waves, the total change in distance between the source and detectors was three times higher when the detectors were directly above the waves, and for 6-in waves, the total change in distance was almost two times higher when the detectors were placed closer to the waves. In the upper detectors, count rates increased with increasing wave size. For 3-in waves, count rates continuously increased as the detectors were moved further from the neutron source. Count rates above 9.00-in and 12.00-in waves increased when the detectors were above the trough of a wave and then decreased again as the detectors moved over a wave peak.

5.2 Moving Source Simulations

Additional MCNP simulations were run modeling moving sources. Both 4-detector configurations were used for this experiment, with the cadmium sheet placed between the polyethylene blocks and placed 1.00 in (2.54 cm) above the water surface, which was flat. A

source was either placed 1.00 in (2.54 cm) above the surface of the water and of even height with the center of the detectors, or 1.00 in (2.54 cm) below the surface. Because MCNP cannot simulate moving sources, a series of stationary sources were evenly spaced along lines. These stationary count rates were then converted into the maximum velocity at which a boat could be traveling and count rates would still be above background. The source was moved in both the x and y directions to compare the detector response. Figure 37 shows the setup for both parallel and perpendicular detectors.

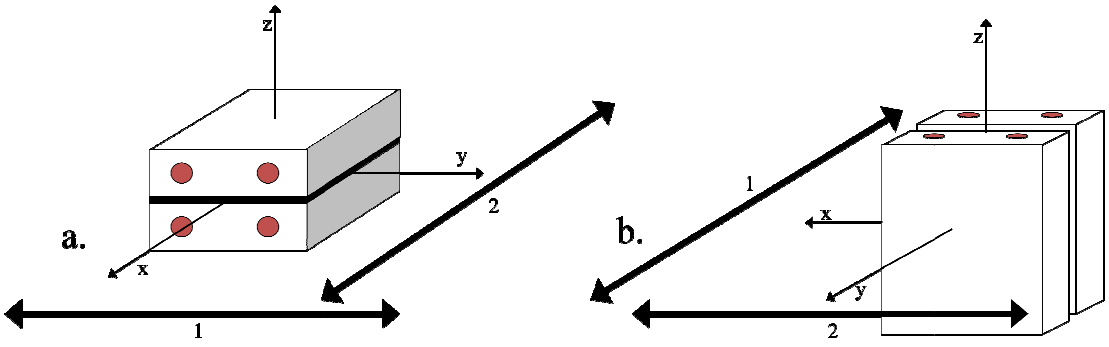

Figure 37. The moving sources for parallel detectors (37a) and perpendicular detectors (37b). Line 1 represents sources at a constant distance x moving in the y direction while line 2 represents sources moving in the x direction at a constant distance y from the detectors.

5.2.1 Moving Sources with Parallel Detectors

Figure 38 compares the detector response for the parallel detectors for sources moving in the x-direction. The source was held a constant distance of 1.00 ft, 2.00 ft, or 3.00 ft in the y-direction from the detectors, and the source was placed at 3.00-in intervals along this line in the positive x direction. The source was initially placed either along the x-axis, for sources moving in the y direction, or on the y-axis for sources moving in the x direction. This was called

position 0. Figure 39 compares the parallel detector response for sources moving in the y direction.

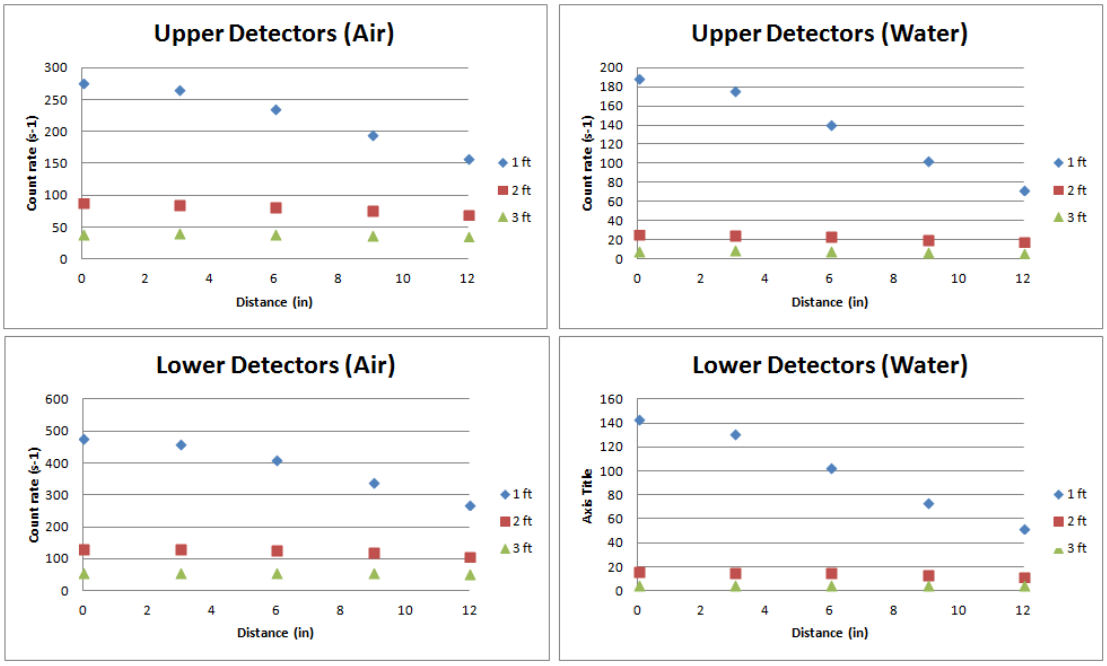

Figure 38. Parallel detector response to a source either in the air or under water moving in the x direction.

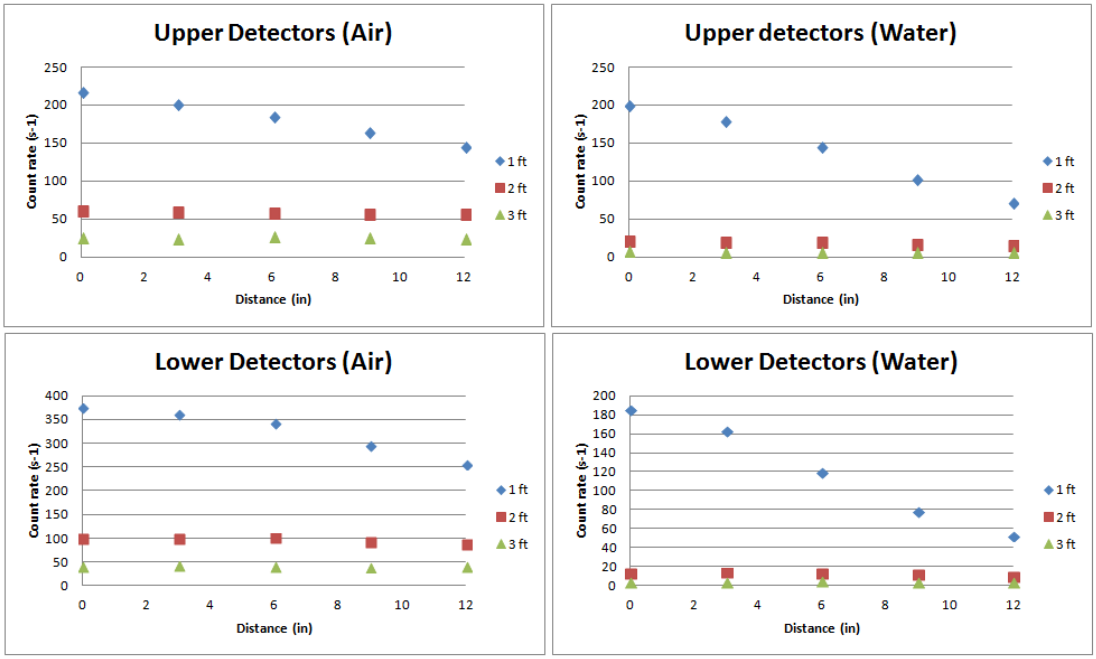

Figure 39. Parallel detector response to a source either in the air or under water moving in the y direction.

Count rates were noticeably higher in the air; count rates in the lower detectors were three times higher with the source in air than in the upper detectors. Count rates dropped off more precipitously when the source was only placed 1 ft away from the detectors; this is for the same reason as explained in Section 5.1.4. With the source on a line closer to the detectors, the 3-in movement of the source resulted in a greater increase in distance from the detectors than that same movement on a line further from the detectors.

Count rates were initially higher for sources moving in the y-direction, but dropped off more quickly as the source moved farther from the initial position. Sources moving in the x-direction were moving parallel to the cylindrical detectors, so the detector area presented to the source was large and remained relatively constant as the source was moved. Conversely, when the source was moving in the y-direction, the source was passing by the ends of the detectors, and a smaller surface area of the detector was presented to the source.

Table VIII compares the maximum detectable velocities for one SQ of weapons grade plutonium moving along each line. The velocity was obtained by multiplying each count rate by a time step Δt to determine the total counts that would be recorded for a source at that location. Each of these counts was summed to determine the total number of counts recorded. The velocity was obtained by dividing the distance the source traveled by the total time the source was in this distance. The velocity was increased until the counts dropped below 1.5 cps, which is 3σ above background, as this is the typical alarm threshold.

Table VIII. Maximum detectable velocities for sources moving in a line 3.00 ft away from the parallel detectors.

Line	X direction		Y direction	
	Air	Water	Air	Water
3 ft	32.6	5.8	50	7.0

For sources passing directly by the detectors, the maximum velocity was very high. Even though the source was only passing by the detectors for a short time, the source was close enough that count rates were high enough to compensate. The maximum velocity was lower for sources under water than in air; this is because of the moderation of the water. Neutrons born in the water are moderated before they can leave the water, reducing count rates. The maximum detection velocity was also higher when the sources were moving in the x-direction (at a constant distance y), again due to the greater detector surface area facing the source, resulting in higher count rates.

5.2.2 Moving Sources with Perpendicular Detectors

The 4-detector perpendicular configuration was also simulated with moving sources in the x and y directions. Sources were again placed on lines 1.00 ft, 2.00 ft, and 3.00 ft away from

the detectors, with a 3.00-in spacing between source locations. Figure 40 shows the detector responses for sources moving in the x-direction while Figure 41 shows detector responses for sources moving in the y-direction.

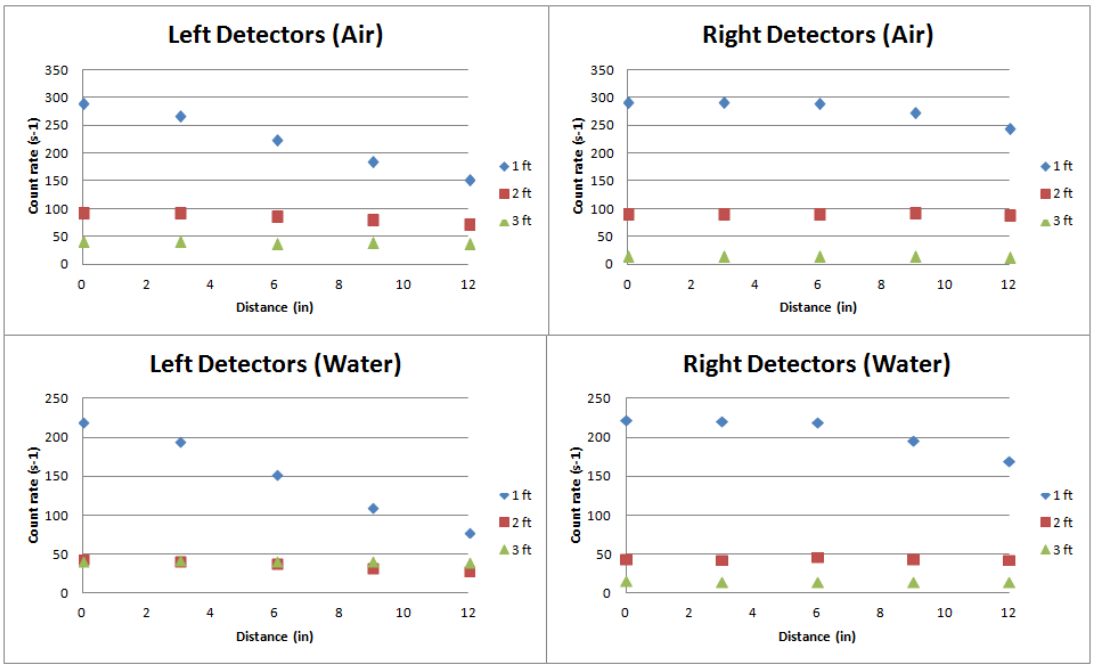

Figure 40. Perpendicular detector responses to a source either in the air or under water moving in the x direction.

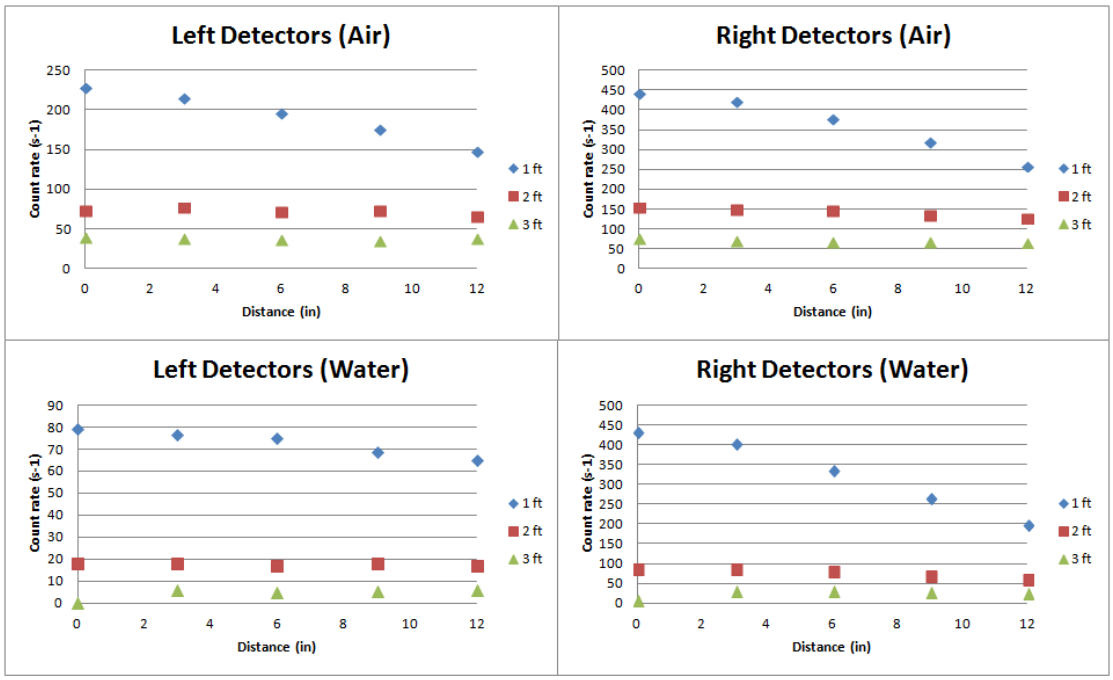

Figure 41. Perpendicular detector responses to a source either in the air or under water moving in the y direction.

Count rates in the perpendicular detectors were higher with a source moving in the y-direction than in the x-direction. With the source moving in the y-direction, it moved closest to the side of the right detectors, resulting in much higher count rates in the right detectors than the left detectors. The count rates in the right detectors were twice as high as count rates in the left detectors for sources in air, and five times higher for sources in water. For sources 2.00 ft or 3.00 ft away, the count rates did not drop precipitously as they did for source moving only 1.00 ft away. For sources moving in the x-direction, the count rate initially started the same in both left and right detectors, as the source was equidistant between the detectors. The source moved closer to the right detectors, resulting in a steep drop in the count rates in the left detectors and a more gradual drop in counts in the right detectors.

The perpendicular configuration outperformed the parallel configuration in some instances. With sources in the air moving in the y-direction, count rates were higher for

perpendicular detectors. This is likely because, with a source in this position, the source was closest to the ends of the detectors in the parallel configuration and closest to the long cylindrical side of the detector in the perpendicular configuration. The greater detector area presented by the perpendicular detectors resulted in higher count rates. Conversely, with sources moving in the x-direction, count rates in the parallel detectors were higher than count rates in the perpendicular detectors. Here, a greater surface area was presented by the parallel detectors. The perpendicular detectors also recorded marginally higher count rates for sources moving under water. Even though the parallel configuration as better able to detect sources placed directly under the detectors, sources placed a greater lateral distance from the detectors were better detected by the perpendicular detectors. The increased distance allowed for a greater surface area of the perpendicular detectors to be exposed to the source.

Table IX compares the maximum velocities for sources moving past perpendicular detectors. For sources passing directly by the detectors, the maximum velocity was again very high. Similar to sources moving past the parallel detectors, the maximum velocity was lower for sources under water than in air; this is because of the moderation of the water. The maximum detection velocity was also higher when the sources were moving in the y-direction due to the greater detector surface area facing the source, resulting in higher count rates. The maximum detection velocity was higher for perpendicular detectors than parallel detectors for all positions except sources moving in the x-direction in the air.

Table IX. Maximum detectable velocities for sources moving in a line 3.00 ft away from the perpendicular detectors.

Line	X direction		Y direction	
	Air	Water	Air	Water
3 ft	48	7.8	50	18

6. CONCLUSIONS

The detector configuration experiments run at the NSC and simulated in MCNP showed that the 4-detector parallel configuration was the best configuration tested overall for detecting sources close to the detectors. Both 4-detector configurations provided directional information on the location of the neutron source, which the 2-detector configurations could not. The parallel configuration recorded higher count rates for the source locations tested. Adding a cadmium sheet between the polyethylene blocks was found to increase the ratio of counts between the lower and upper detectors, providing greater directional information on the location of a source.

Additional simulations showed that count rates fluctuated when a source was placed in a wave. With count rates taken at eight equally spaced locations in a wave period, the count rates did not average out to the count rate above flat water. With the detectors placed in a parallel configuration directly above the waves, the count rates were lower above waves than above a flat plane of water, and count rates dropped as wave size increased. The upper detectors were better able to detect sources over waves than over flat water, but count rates were much lower than in the lower detectors. Raising the detectors to a greater height minimized the impact of the waves on count rates, but resulted in a large decrease in count rate. Additionally, for sources moving relative to the detectors, the environment the source was surrounded by, be it water or air, had a greater effect on count rates than the distance between the source and detector.

Modeling a moving source revealed that a source under water could be detected in a boat moving at velocities up to 18 kts when moving in the y-direction in a line 3 ft away from the perpendicular detectors and only 7.8 kts when moving in the x-direction. The maximum detectable velocity for these same sources with the parallel detector configuration was only 5.8

kts in the x-direction and 7 kts in the y-direction. Even though the 4-detector parallel configuration was better at detecting sources close to the detectors, the perpendicular configuration could detect sources placed farther from the detectors.

Future work includes experimental validation of the simulations. A wave pool could be used to experimentally produce waves of a specific height and period. By using a pool to control the size of the waves created, this variable could be isolated and the effects of wave size on detection count rates can be independently verified. Additional tests to confirm the maximum detection velocity should be performed. With the appropriate permissions, this could be performed at a lake such as the one at Disaster City, which allows for radioactive sources.

REFERENCES

1. International Atomic Energy Agency. “IAEA Illicit Trafficking Database.” http://www-ns.iaea.org/downloads/security/itdb-fact-sheet.pdf (accessed November 15, 2012).

2. B. Hoffman, B. Claridge, and D. Claridge. *Illicit Trafficking in Nuclear Materials*. University of Michigan, United States: Research Institute for the Study of Conflict and Terrorism (1999).

3. International Atomic Energy Agency. "Measures to Prevent, Intercept and Respond to Illicit Uses of Nuclear Material and Radioactive Sources." Stockholm, 2002. http://www-pub.iaea.org/MTCD/Publications/PDF/CSP-12-P_web.pdf (accessed 15 November 2012).

4. Embassy of the United States. “Remarks of President Barack Obama.” April 5, 2009. http://prague.usembassy.gov/obama.html (accessed October 3, 2012).

5. National Nuclear Security Administration. "Fact Sheet: NNSA’s Second Line of Defense Program." February 1, 2011. https://nnsa.energy.gov/mediaroom/factsheets/ (accessed 9 October, 2012).

6. International Atomic Energy Agency. "IAEA Safeguards Glossary." Vienna, 2002. http://www-pub.iaea.org/MTCD/publications/PDF/nvs-3-cd/PDF/NVS3_prn.pdf (accessed 12 November 2012).

7. Department of Homeland Security. "Small Vessel Security Strategy." April 2008. http://www.dhs.gov/xlibrary/assets/small-vessel-security-strategy.pdf (accessed 26 November 2012).

8. R.C. Byrd et al. “Nuclear Detection to Prevent or Defeat Clandestine Nuclear Attack.” *IEEE Sensors J* 5.4 (2005): 593-609.

9. D. Reilly, N. Ensslin and H. Smith (Ed.), *Passive Nondestructive Assay of Nuclear Materials*. First Edition. Washington DC: United States Nuclear Regulatory Commission (1991).

10. P. Goldhagen. “Experimental Study of the Neutron Ship Effect.” *Environmental Measurements Laboratory Annual Report — FY 2004*, EML 625 (2005): 9-10.

11. K. P. Ziock. "Autonomous Radiation Monitoring of Small Vessels." *Nuclear Instruments and Methods A* 652 (2011): 10-15.

12. N.M. Johansen III, *An Active System for the Detection of Special Fissile Material in Small Watercraft.* MS Thesis Texas A&M University, 2006. College Station. Print.

13. R.J. Sheu et al. "A Study of the Cosmic-ray Neutron Field Near Interfaces." *Nuclear Instruments and Methods A* 476 (2002): 52.

14. K. O'Brien et al. "Cosmic-Ray Induced Neutron Background Sources and Fluxes for Geometries of Air Over Water, Ground, Iron, and Aluminum." *Journal of Geophysical Research-Space Physics* 83 (1978), 114-120.

15. R.T. Kouzes et al. "Cosmic-ray-induced Ship-effect Neutron Measurements and Implications for Cargo Scanning at Borders." *Nuclear Instruments and Methods in Physics Research Section A* 587 (2009): 89-100.

16. R.T. Kouzes et al. "Passive Neutron Detection for Interdiction of Nuclear Material at Borders." *Nuclear Instruments and Methods in Physics Research Section A* 584 (2008): 383-400.

17. R.T. Kouzes, et al. "Neutron Detection Alternatives to ^{3}He for National Security Applications." *Nuclear Instruments and Methods in Physics Research Section A* 623.3 (2010): 1035-1045.

18. Nuclear Data Center. "Online Plotter for MCNP and ENDF Cross Section Data." http://atom.kaeri.re.kr/cgi-bin/endfplot.pl. (accessed 24 November 2012).

19. D.B. Pelowitz et al. "MCNPX User's Manual, Version 2.7.0." LA-CP-11-00438, April 2011.

20. LND Inc . "Cylindrical ^{3}He Neutron Detector." http://www.lndinc.com/products/538/ (accessed 23 September 2012).

21. S. Roesler et al. "Calculation of Radiation Fields in the Atmosphere and Comparison to Experimental Data." *Radiation Research* 149 (1998): 87.

22. B. Wiegel et al. "Spectrometry Using the PTB Neutron Multisphere Spectrometer (NEMUS) at Flight Altitudes and at Ground Level." *Nucl. Instr. and Meth. A* 476 (2002): 52.

23. M. Yamashita et al. "Cosmic-ray-produced Neutrons at Ground Level: Neutron Production Rate and Flux Distribution." *Journal of Geophysical Research* 71 (1966): 3817.